Sustainable Energy & Fuels

REVIEW

View Article Online
View Journal | View Issue

Cite this: *Sustainable Energy Fuels*, 2017, **1**, 1475

H_2/O_2 enzymatic fuel cells: from proof-of-concept to powerful devices

I. Mazurenko, X. Wang, A. de Poulpiquet and E. Lojou *

Intensive research during the last 15 years on mechanistic understanding of hydrogenases, the key enzyme for H_2 transformation in many microorganisms, has authorized the concept of green energy production through H_2/O_2 enzymatic fuel cells (EFCs), in which enzymes are used as biodegradable and bioavailable biocatalysts. More recently, great effort has been put in the improvement of the interfacial electron transfer process between the enzymes and high surface area conductive materials in order to shift from a proof-of-concept to a usable power device. Herein, we analyze the main issues that have been addressed during the last 5 years to make this breakthrough. After a brief introduction on the structure of hydrogenases and bilirubin oxidases, a widely used enzyme for O_2 reduction, we compare their activity with that of platinum. We introduce the first H_2/O_2 EFCs and discuss their main limitations mainly related to the sensitivity of hydrogenases to O_2 and oxidative potentials. We then review the discovery of new enzymes in the biodiversity and the advances in the control of the functional immobilization of these enzymes on electrodes that have permitted to overcome these limitations. We finally present all the reported H_2/O_2 EFCs, with a critical discussion on the perspectives of such devices.

Received 6th April 2017
Accepted 5th June 2017

DOI: 10.1039/c7se00180k

rsc.li/sustainable-energy

Introduction

Two years ago, within COP21, 195 countries adopted a first universal deal aiming at maintaining the global average temperature increase below 2 °C (source: https://unfccc.int/resource/docs/2015/cop21/eng/10a01.pdf). This ambition requires a transition from non-renewable carbon-based energy sources to clean and low-carbon energy sources. The emergence of renewable energy sources such as solar and wind ones also induces the need of sustainable energy carriers that would allow to deliver and store this energy notably during intermittent

Aix Marseille Univ, CNRS, Bioénergétique et Ingenierie des Protéines, 31 Chemin Joseph Aiguier, 13009 Marseille, France. E-mail: lojou@imm.cnrs.fr

Elisabeth Lojou is a senior researcher in the Bioenergetic and Protein Engineering Laboratory (Aix Marseille University, CNRS) in France. Her group develops research in the domain of fundamental bioelectrochemistry, with a special interest in the electron transfer between functionalized nanostructured electrodes and redox enzymes, such as hydrogenases and multicopper oxidases. Since 5 years, it is engaged in the design of H_2/O_2 enzymatic fuel cells.

From left to right: ***Xie Wang*** *is a biochemist working as a second year PhD student on the energy metabolic chain of an acidophilic bacterium;* ***Ievgen Mazurenko*** *is a post-doctoral researcher. He obtained his joint PhD degree from the University of Lorraine (Nancy, France) and the Taras Shevchenko National University of Kyiv (Ukraine) in 2013. His research interests involve electrochemistry, nanomaterials and immobilized biomolecules with a view to designing various biodevices for energy and substance conversion;* ***Elisabeth Lojou****;* ***Anne de Poulpiquet*** *obtained her PhD degree at Aix-Marseille University (France) under the direction of Dr Elisabeth Lojou. After a postdoctoral at the Institute of Molecular Sciences in Bordeaux (France), she joined the Bioenergetic and Protein Engineering Laboratory as an assistant professor. Her research interests focus on coupling electrochemistry to optical techniques to study the electro-enzymatic reactivity.*

production. Hydrogen meets this requirement, presenting at the same time high energy density and harmless water generation upon reaction with abundant oxygen. Hydrogen can be produced from clean energy sources such as biomass, and is transportable either in a liquid or gas state, or combined with nanomaterials. H_2 high energy conversion efficiency in fuel cells (above 60%) is one last applicative interest of this fuel. With all these advantages, is the competition with Li batteries the unique reason for slow development of H_2-based fuel cells, especially for transportation? One drawback of proton exchange membrane fuel cells (PEMFCs) is that they rely on the requirement for catalysts, mainly based on noble metals such as platinum, to accelerate the reactions of H_2 oxidation and O_2 reduction. Pt use encounters availability, economic and political issues. During the last few decades, active research thus focused towards the decrease or even the replacement of Pt in fuel cells. Can we imagine enzymes doing the job? In microorganisms, enzymes are biocatalysts that very efficiently convert various substrates, *e.g.* to sustain microorganism energy. The identification, then purification, and finally immobilization on electrodes of some of these enzymes led to the concept of enzymatic fuel cells (EFCs), which would operate as PEMFCs, but with biocatalysts harboring only earth-abundant metals and offering a larger panel of available fuels and oxidants[1] (Fig. 1). Actually, EFCs based on substances largely available in physiological fluids, such as glucose and O_2, associated with the specific enzymes, *i.e.* glucose oxidase and multicopper proteins such as bilirubin oxidase (BOD), were the most developed systems since their proof of concept in 1964.[2–4] Powering of medical devices was targeted with implanted EFCs, or more recently with systems disposed on lenses or on patch applications.[5–9] Interest in the development of H_2/O_2 EFCs is much more recent, and motivated by the expected high energy output and applications in the powering of portable electronics.[10,11]

In H_2/O_2 EFCs, hydrogenase, first recognized in 1931, is the key enzyme for H_2 oxidation at the anode.[12] However, H_2/O_2 EFCs were developed late compared with glucose/O_2 EFCs, mainly because of the extreme oxygen sensitivity of most hydrogenases. Extensive research during the last decade towards the understanding of O_2 sensitivity of hydrogenases and the discovery of new hydrogenases presenting outstanding properties including O_2 tolerance and CO resistance, nowadays permit the envisioning of the development of H_2/O_2 EFCs.

This literature survey provides an excellent opportunity to emphasize the most recent improvements and breakthroughs in the knowledge of the involved enzymes in H_2/O_2 EFCs, in rational use of (nano)materials as the enzyme host matrix, in understanding of the interactions between these materials and enzymes required for fast electron transfer, and then in the resulting high power output of the related devices. It also allows to identify the remaining bottlenecks and future fundamental research directions required in this domain to fulfill the application requirements.

The proof-of-concept

The first H_2/O_2 enzyme-based fuel cell was not an entirely enzymatic one. Nevertheless, it was an initial proof that electricity could be generated by microorganisms presenting H_2 metabolism, opening the way for a true H_2/O_2 EFC. Actually, Tsujimura *et al.*[13] reported in 2001, *i.e.* 70 years after the discovery of hydrogenase activity in bacteria, a fuel cell based on sulfate-reducing cells at the anode and BOD at the cathode, both deposited on 0.22 cm^3 carbon felts. Methyl viologen (MeV) and 2,2′-azinobis(3-ethylbenzothiazoline-6-sulfonate) (ABTS) redox mediators were used to mediate H_2 oxidation and O_2 reduction respectively. The fuel cell operated at 1.0 V with a current of 0.9 mA, exhibiting the highest open circuit voltage

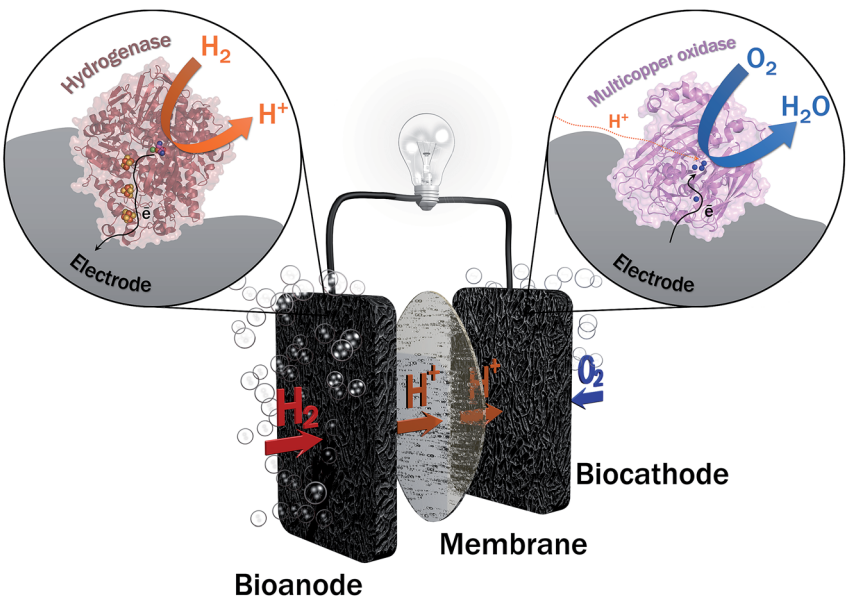

Fig. 1 General scheme of the H_2/O_2 EFC. At the anode hydrogenase is the enzyme for H_2 oxidation. Multicopper oxidase such as BOD reduces O_2 into water at the cathode. A proton exchange membrane eventually separates the two compartments.

(OCV) ever reported for EFCs of 1.17 V. In this hybrid bacterial/enzymatic H_2/O_2 fuel cell, the anode activity towards H_2 oxidation was suggested to be linked to the hydrogenase content of the periplasmic space of *Desulfovibrio vulgaris* Hildenborough (*Dv*H). In our group, we further demonstrated that *Dv*H was able to communicate with a pyrolytic graphite electrode (PG) in the presence of MeV in solution, exhibiting H_2 oxidation or proton reduction activity depending on pH.[14] The activity was measured with whole cells and periplasmic, membrane or cytoplasmic fractions, where different hydrogenases were identified. The highest contribution of the periplasmic hydrogenase in the overall catalytic current, and more specifically in the H_2 uptake direction was proposed.[15] Actually, H_2 metabolism is widespread in many biotopes and in very different microorganisms. It is supported by the presence of many various hydrogenases. The occurrence of microorganisms gaining energy from H_2 in air early suggested that some hydrogenases could even operate at high O_2 concentrations.[16] Hydrogenases differ in the metal content of the active site, which can be composed of Fe only, di-Fe or Ni and Fe atoms.[17,18] Most often both [FeFe]- and [NiFe]-hydrogenases are identified in a given cell. They are located in different spaces and present a bias toward H_2 uptake or evolution. Some of them have been recognized to be bidirectional and able to perform electron bifurcation to harness energy.[19] In *Desulfovibrio fructosovorans* (*Df*), another sulfate-reducing bacterium, 6 different hydrogenases were identified in the genome! This indicates a complex but very efficient machinery that may be exploited in EFCs.

Turning from bacterial cells to enzymes

Among the three classes of hydrogenases, *i.e.* [FeFe], [NiFe] and [Fe] hydrogenases, the [FeFe] hydrogenase presents the highest turnover rate for H_2 evolution/uptake. Nonetheless, the [NiFe]-hydrogenase is the most wide-spread. It is present in all *Proteobacteria* as well as in *Firmicutes*, *Cyanobacteria*, *Aquificae*.[19] It is also the most robust hydrogenase especially towards O_2-tolerance, and its role in the microorganism is H_2 uptake.[17,18,20–22] Therefore, this class of hydrogenases is the most adapted for use in EFCs.

[NiFe]-hydrogenases share a similar overall structure.[18] The enzyme is composed of two subunits (Fig. 2). In addition, the membrane-bound [NiFe]-hydrogenases have a trans-membrane helix that serves as an anchor to the membrane. The large subunit harbors the [NiFe] active site, in which the Fe ion is coordinated by 1 CO and 2 CN^- ligands, while two cysteine residues bridge the Ni and Fe atoms. A conserved pendant arginine would also act as a catalytic base for H_2 activation.[23] The small subunit contains three FeS clusters at a distance less than 13 Å and is able to transfer electrons from the active site to the physiological partner. Gas diffusion channels allowing H_2 to reach the active site are identified. Nowadays, in-depth biochemical and spectroscopic characterization of [NiFe]-hydrogenases from different organisms allows to propose a global mechanism for H_2 oxidation[18,21] (Fig. 2). In brief, H_2 reaches the Ni(II)Fe(II) active site (known as Ni-SI state) where it undergoes heterolytic cleavage resulting in a Ni(II)Fe(II) state with H^- bridging the two atoms. Successive release of 2 protons and 2 electrons leads back to the initial Ni(II)Fe(II) state. However, some debates subsist concerning inactive states of the enzyme.[24]

Concerning O_2 reduction, multicopper oxidases (MCOs) have been reported for many years as efficient bioelectrocatalysts reducing O_2 into water.[25–28] Laccase and BOD belong to this class of proteins, and they are found in many fungi and bacteria. They are both commonly used in sugar/O_2 EFCs.[4] However, BOD tends to surpass laccase because it is able to operate at neutral pH and is less sensitive to chloride at this pH.[29] BOD contains four copper atoms, which are classified according to their geometric and spectroscopic properties: one T1 Cu, one T2 Cu coupled to a binuclear T3 Cu (the TNC center) (Fig. 3). As for hydrogenases, the global catalytic cycle is determined, although some states remain unclear, especially those formed in the presence of halides[30–32] (Fig. 3). Briefly, O_2 binds at the TNC center of the fully reduced BOD, and is reduced into water following two successive electronic steps involving a peroxy state and a state where a hydroxyl bridges the T3 copper atoms.[27,28,33] The electrons are received at the T1 Cu and transferred to the TNC through a conserved (His-Cys-His) sequence.

Replacing platinum with enzymes?

The first report that envisioned hydrogenase as a biocatalyst in replacement of Pt is dated 1977.[34] This was encouraged by the demonstration of hydrogenase ability to exchange electrons with an electrochemical interface to oxidize H_2, at least with the aid of a redox mediator. This type of electron transfer process is named Mediated Electron Transfer (MET). At that time, the possibility of direct connection (Direct Electron Transfer (DET)) between the active site of the enzyme and the electrode was an open question[34] (Fig. 4). DET between proteins less than 20 kDa and various electrodes was known since the 1970's.[35] The issue of required orientation to expose the metal center close to the electrode was also clearly identified. However, the burying of the active site into the protein moiety of larger enzyme molecules (more than 50 kDa and 5 nm diameter if considered as globular) was long believed to preclude any DET. Until now, MET is still widely used to connect enzymes *via* small redox molecules either diffusing or immobilized mostly within polymers at the electrode.[36,37] Many enzymes are still not directly addressable by electrochemistry. However, some of them, including hydrogenases and bilirubin oxidases, have been proved to be able to directly exchange electrons with electrodes such as pyrolytic graphite electrodes (PG).[38,39] Before deeper explanations, which will be exposed later in this review, it was suggested that some enzyme molecules were able to adopt a favorable orientation for DET, *i.e.* placing the surface FeS (distal cluster) or Cu T1 at a tunneling distance from the electrode, for hydrogenase and BOD respectively. In the DET process, enzymatic rates are then measured directly as a current.

The successful direct electric communication of enzymes on electrodes allowed comparison with Pt, a prerequisite towards further H_2/O_2 EFC developments. Accordingly, O_2 reduction by the Pt electrode was compared to BOD immobilized on an

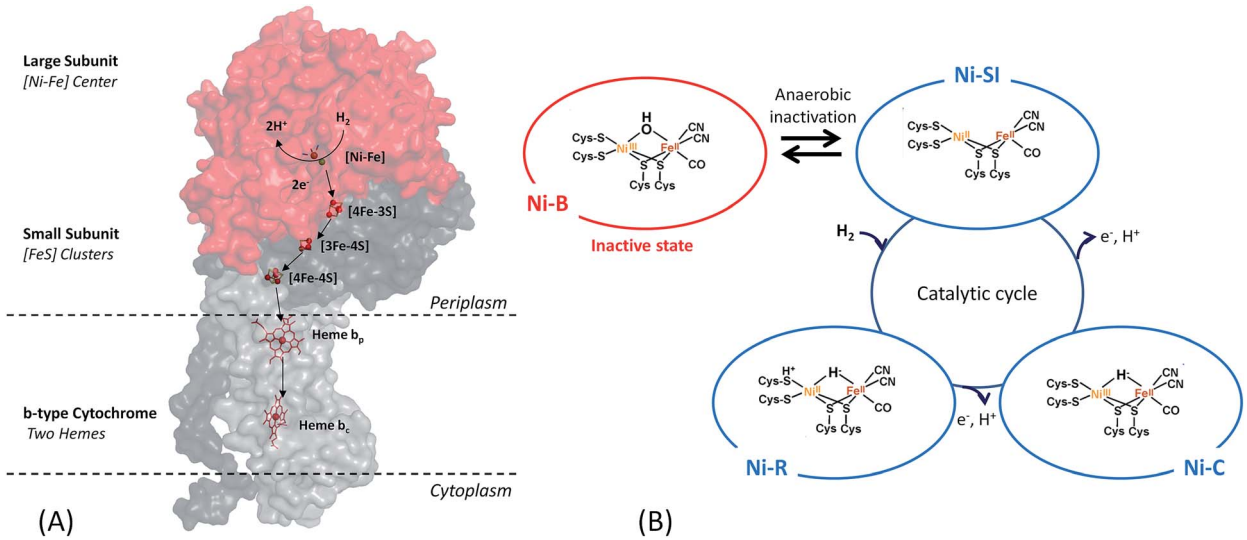

Fig. 2 O_2-tolerant [NiFe]-hydrogenases are key enzymes for H_2 oxidation. (A) Structure of membrane-bound [NiFe]-hydrogenase showing the large subunit and the small subunit harboring the [NiFe] active site and the 3 FeS clusters, respectively, as well as the trans-membrane helix. Electron pathway from the [NiFe] active site through the FeS clusters and the diheme cytochrome *b* partner is also drawn. (B) States of the [NiFe]-hydrogenase involved in the catalytic cycle for H_2 oxidation and Ni-B state formed at high potential in the absence of oxygen.

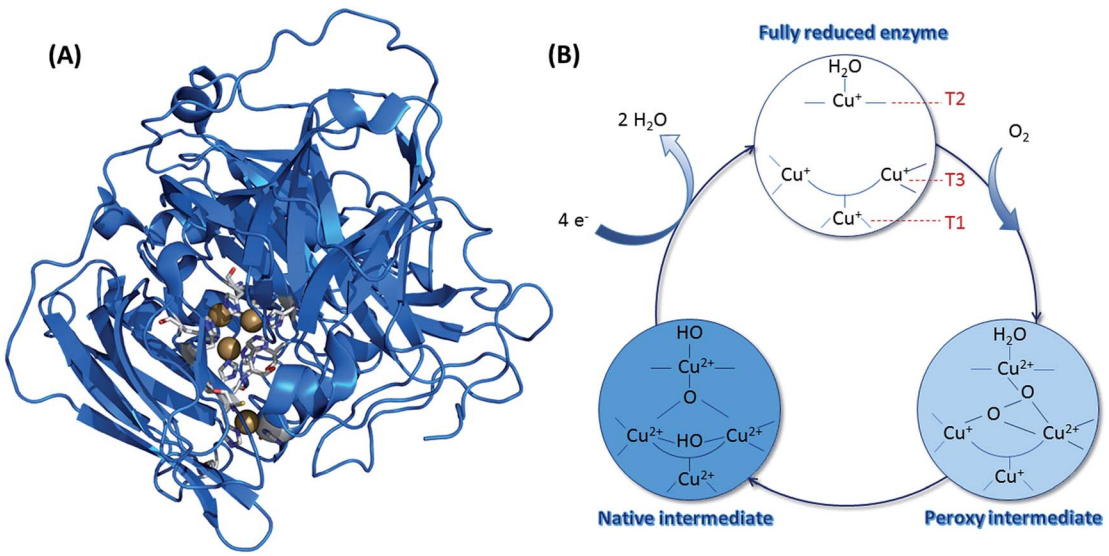

Fig. 3 (A) Crystal structure of BOD from *Myrothecium verrucaria* (PDB ID: 2XLL). Copper atoms are represented by brown spheres, and their ligands appear as sticks with colors corresponding to the elements. Color code: white: carbon; blue: oxygen; red: nitrogen and yellow: sulfur. (B) Catalytic cycle involved in the mechanism of O_2 reduction by BODs, with the different redox states of the three Cu atoms.

electrode. An accurate comparison is complicated by the most often unknown quantity of enzyme participating to the current. However, based on an electroactive enzyme monolayer, the electrochemical data suggested that the enzyme should be several orders of magnitude more efficient than Pt.[40–42] Net improvement in the overpotential required for O_2 reduction was also expected by using BOD which has been maturated for bilirubin oxidation; hence presenting a high potential T1 Cu.[43] Actually, the overpotential of O_2 reduction was shown to be much lower for the enzyme compared to that of Pt, especially at neutral pH or moderate acidic pH.[40,42] For BOD from the fungus *Myrothecium verrucaria* (*Mv*), an overpotential of 80 mV was measured at pH 5 against 210 mV for Pt under the same pH conditions. It should be also underlined that BOD outperformed Pt in complex media, for example, in air-saturated human blood.[42] These results confirm the previous conclusion drawn from comparative O_2 reduction efficiency between Pt and BOD wired in redox hydrogels.[5,44] In this latter case, the enzyme loading is also far above the monolayer, allowing the envisioning of current densities in the same range as Pt-loaded carbon nanoparticles.

[NiFe]-hydrogenase from *Allochromatium vinosum* (*Av*) adsorbed on PG at 45 °C was compared to Pt under the same

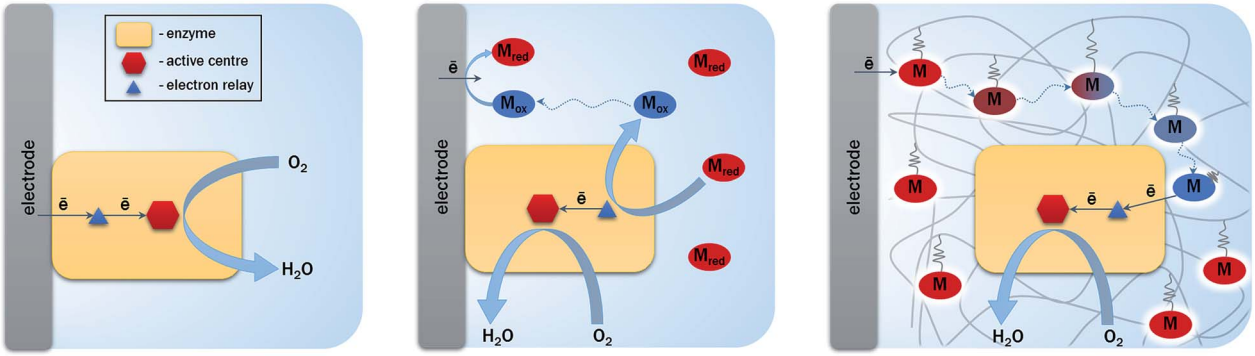

Fig. 4 Electrocatalysis using enzymes proceeds either *via* a direct enzyme connection at the electrode (DET, left), or through a redox mediator (MET) either diffusing (middle) or immobilized for example in hydrogels (right).

conditions.[45] Under 1 atm H_2, a similar catalytic current for H_2 oxidation was recorded between the hydrogenase and Pt at an overpotential of 200 mV. The absence of non-catalytic signal for the hydrogenase precluded any quantification of the enzyme coverage. However, the similarity of current between the enzyme and Pt suggested a higher turnover rate for the enzyme to compensate for the low density of catalytic sites. At lower overpotentials, the enzyme was progressively less efficient as a result of interfacial and intramolecular electron transfer limitations, except when low H_2 concentrations were used. It was also demonstrated that the enzyme surpassed Pt in the presence of CO. While CO immediately poisoned Pt, the hydrogenase recovered its activity after CO removal. The comparable efficiency of hydrogenase over Pt was confirmed later by Karyakin *et al.*, even when the Pt-based electrode was operating under sulphuric acid condition.[46] Woolerton *et al.* finally compared the efficiency of the membrane-bound hydrogenase from the aerobic bacterium *Ralstonia eutropha* (*Re* MbH) and that of Pt for oxidation of low levels of H_2.[47] Interestingly it was shown that the extremely high affinity of hydrogenase towards H_2 (K_M = 6 μM) resulted in the enzyme outperforming Pt for sub-atmospheric H_2 levels. H_2 oxidation was even recorded in mixtures of H_2 and O_2, under conditions where most hydrogenases were expected to be inactivated. An inactivation process of hydrogenase at high potentials, not occurring on Pt, limited however the usable potential range. Electrochemical data underlined that both the enzyme-based and Pt-based electrodes oxidized H_2 and reduced O_2, albeit the enzyme was much more efficient in H_2 oxidation, thus again outperforming Pt in H_2/O_2 gas mixtures. At the same time, progressive inhibition of *Re* MbH by O_2 was demonstrated. A fast recovery of the activity was however noticed after O_2 removal, suggesting an O_2-tolerance of this enzyme extracted from an aerobic bacterium. Last but not least, the *Re* MbH-based bioanode was demonstrated to be insensitive to CO.

The first enzymatic H_2/O_2 EFCs

Based on the efficiency of hydrogenases and MCOs, and on the ability of *Re* MbH to operate in air, the first H_2/O_2 EFC with no membrane separator was designed by Vincent *et al.* in 2005.[48] The EFC operated at 30 °C, pH 5.6 in a beaker containing buffer flushed with H_2 close to the bioanode, and air close to the biocathode. *Re* MbH and a laccase were deposited on graphite strips of 0.7 cm^2. The OCV was 970 mV, and a maximum power of 5 μW was reached. Comparison with an EFC running with the hydrogenase from *Av* showed a maximum power of 0.2 μW.[48] In addition to provide the proof that hydrogenase could be coupled to MCO in a H_2/O_2 EFC to produce electricity, this paper also underlined the requirement of an O_2-tolerant hydrogenase, such as the membrane-bound [NiFe]-hydrogenase from *Re*. Afterwards, another H_2/O_2 EFC was demonstrated to be able to operate in 3% H_2 in air, thanks to the peculiar properties of the membrane-bound hydrogenase from *R. metallidurans*.[49] An OCV of 950 mV and a maximum power density of 5.2 μW cm^{-2} were recorded. Three cells in series were shown to power a wristwatch for 24 h. Even if a low power density was obtained due to very low enzyme coverage on graphite, these results clearly highlighted the great potential of such devices based on high H_2 affinity, O_2-tolerant MbH hydrogenases and high redox potential MCO.

Limitations of the first H_2/O_2 EFCs

The initial biodevices also put forward the main limitations that had to be overcome in view of large scale development of H_2/O_2 EFCs. The first prerequisite is the use of efficient but stable enzymes. The anodic side which relies on sensitive hydrogenases is especially critical. The identification of the O_2-tolerant *Re* MbH opened the route for new outstanding enzymes. This is the case of the membrane-bound [NiFe]-hydrogenase from *Escherichia coli* (*Ec*Hyd1) which was proved to be very active for H_2 oxidation in air.[50] O_2-tolerance is not sufficient however. Wait *et al.* pushed forward the understanding of H_2/O_2 EFCs by comparing their performance in three different configurations: (i) fuel cell with a Nafion membrane separator fed with 100% H_2 and 100% O_2 in the anodic and cathodic compartments, respectively; (ii) a membrane-less fuel cell fed with 96% H_2/4% O_2 mixture; (iii) a membrane-less fuel cell fed with 4% H_2/96% air mixture[51] (Fig. 5). The bioelectrodes were based on *Ec*Hyd1 deposited on PG and *Mv* BOD immobilized at a carboxylic-modified PG. Important features can be extracted from these

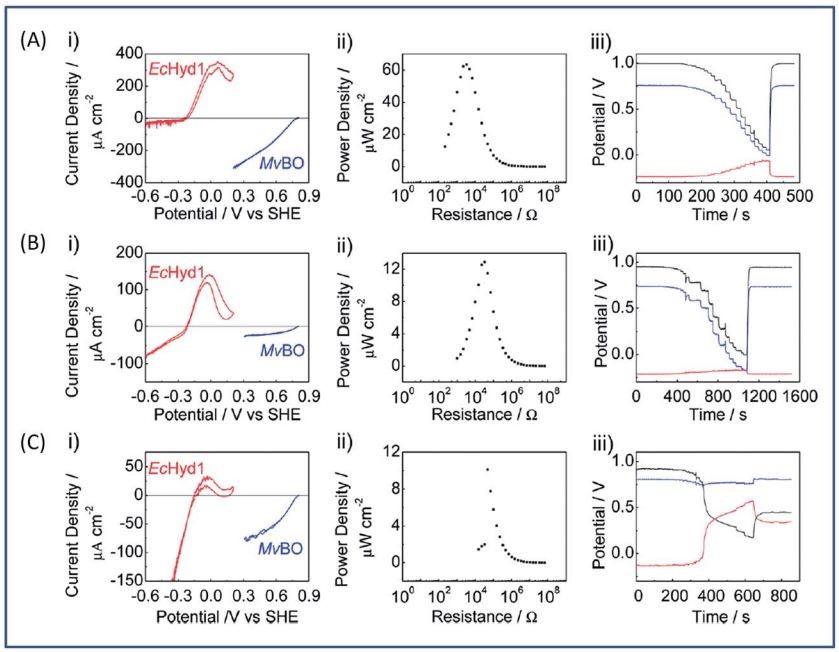

Fig. 5 H_2/O_2 EFC operating in three different configurations and highlighting the effect of hydrogenase inactivation on the EFC performances. (A) Membrane EFC, 100% H_2 and 100% O_2 in the anodic and cathodic compartments; (B) membrane-less EFC, 96% H_2 and 4% O_2 in the anodic and cathodic compartments; (C) membrane-less EFC, 4% H_2 and 96% air in the anodic and cathodic compartments. (i), (ii) and (iii) depict respectively in red catalytic H_2 oxidation by *Ec*hyd1 and in blue catalytic O_2 reduction by *Mv* BOD, power performances, and voltages of cell (black) and individual electrodes (anode in red and cathode in blue). Reprinted with permission from Wait *et al.*, *J. Phys. Chem. C*, 2010, **114**, 12003–12009. Copyright 2017 American Chemical Society.

studies. In the first configuration, the OCV was 990 mV and the maximum power density was 63 μW cm^{-2} at 511 mV. In the second configuration, as expected, the cathode was limiting the EFC. O_2 reduction at the anode occurred, and inactivation of *Ec*Hyd1 was visible at potentials higher than −200 mV *vs.* Ag/AgCl. Full power was restored after the polarization experiment. Conversely, in H_2-poor gas mixtures (configuration iii) where the anode limited the EFC, complete anode inactivation occurred above −50 mV *vs.* Ag/AgCl, full power was not recovered after the polarization experiment and the anode potential was not restored. Typical characteristics of EFCs in the different configurations were demonstrated to be linked to the formation of the inactive state of the hydrogenase under O_2, the so-called Ni-B state (Fig. 2). Many fundamental studies have been dedicated to the kinetics of formation of this inactive state, in which a hydroxyl bridges the Ni and Fe atoms. It is formed in all the hydrogenases either O_2-sensitive or O_2-tolerant, the difference being a faster reactivation rate under reducing conditions for O_2-tolerant hydrogenases.[50,52] One important conclusion of the EFC study was that Ni-B formation restricts the usage of H_2/O_2 EFCs to high-load devices for which the potential of the anode does not exceed critical values. Hydrogenase inactivation induces however a wider use restriction. Indeed, the Ni-B inactive state is also formed at high potential in the absence of O_2. This state can be fully reactivated under reducing potentials. However above 200 mV *vs.* Ag/AgCl inactivation appears to be irreversible. As a consequence, in case of EFCs limited by the anode, even in the presence of a separator membrane, the very high potential reached by the anode may yield irreversible inactivation of the hydrogenase.[53]

In addition to the main limitation associated with hydrogenase inactivation under O_2 or under oxidizing conditions, the first H_2/O_2 EFCs also raised other critical issues. Tsujimura *et al.* concluded that mass transfer controlled the EFC performances, which could be only overcome by using porous materials as host matrices.[13] Further, although enzymes were suggested to be much more active than Pt to compensate the lower surface coverage,[45] the power reached in the EFCs clearly indicated the need to increase the enzyme coverage per geometric area.

Search in the biodiversity for new enzymes with outstanding properties

This review already underlined the benefit of enlarging the panel of enzymes in order to obtain new electrocatalytic properties. This is the case of the O_2-tolerant [NiFe]-hydrogenases such as *Re* MbH and *Ec*Hyd1 which were proved to support high concentrations of O_2 and to be insensitive to CO. These two properties allowed envisioning of their use in biotechnological devices, which had been quite unexpected for the "standard" sensitive hydrogenases originally purified and studied by electrochemistry. Besides *Re* MbH and *Ec*Hyd1, three more [NiFe]-hydrogenases have been identified presenting the same phenotypes of O_2-tolerance and CO-insensitivity. They are present in bacteria able to sustain energy from an electron transfer chain coupling H_2 oxidation to O_2 reduction. The first

one is extracted from the facultative anaerobe *Salmonella enterica*, and is homologous to *Ec*Hyd1.[54] The second one is purified from the hyperthermophilic bacterium *Aquifex aeolicus* (*Aa* MbH).[55] In addition to O_2- and CO-tolerance, *Aa* MbH was demonstrated to be able to oxidize H_2 on a temperature range from 25 °C up to 85 °C [56,57] (Fig. 6). The last one is purified from the aerobic marine bacterium *Hydrogenovibrio marinus* (*Hm* MbH), and was also shown to be thermostable.[58] As a general rule, O_2-tolerant hydrogenases are membrane-bound enzymes, a membrane cytochrome *b* being their physiological partner (Fig. 2). They present a net bias toward H_2 oxidation against proton reduction, but oxidize H_2 at potentials 100–150 mV higher than "standard" O_2-sensitive hydrogenases, a drawback in view of application in EFCs. Many studies are still dedicated to the understanding of the origin of O_2- and CO-tolerance in view of engineering O_2-tolerant hydrogenases or in order to determine the molecular keys to synthesize biomimetic complexes. The crystal structures of four O_2-tolerant hydrogenases definitely helped in the definition of some molecular determinants explaining the O_2-tolerance.[59–62] They are detailed in recent reviews.[10,18,22,63,64] Briefly, the main exceptional feature of O_2-tolerant hydrogenases compared to sensitive ones is the presence of an unusual [4Fe-3S] cluster close to the [NiFe] active site, coordinated by six cysteines instead of four, providing an electron-rich environment. This peculiar FeS cluster allows complete reduction of O_2 into water, which can be evacuated through specific hydrophilic channels. However, this is not sufficient to totally account for O_2-tolerance. Based on various mutations, specific amino acid residues in the canopy very close to the active site and at the end of the gas channels are also suggested to play a key role in the protection.[23,65,66] The tetrameric structure of O_2-tolerant hydrogenases might also act as a rescue mechanism, enabling electron transfer between inactivated and active monomers.[67]

Biodiversity has been less explored for BODs, perhaps because the identification of BODs themselves already provided the key to overcome halide inhibition encountered by the laccases originally used for O_2 reduction.[29] Note however that the inhibition process of MCOs by halides is nowadays intensively revisited.[30–32] Fungal *Mv* BOD is commercially available and is the most widely studied BOD, although some new BODs emerged such as those isolated from the bacterium *Bacillus pumilus* (*Bp*)[68] and from the fungus *Magnaporthe oryzae*.[69] Both of them were demonstrated to be thermostable, but the reason for such thermostability is not elucidated yet. However, the redox potential of T1 Cu, the entry point of electrons, was shown to be 100 mV lower than that of T1 Cu in *Mv* BOD,[70] a feature that will result in lower OCV in EFCs.

How to address the issue of hydrogenase inactivation at high potentials?

As discussed before, anaerobic hydrogenase inactivation at high potentials restricts the devices that can be powered by H_2/O_2 EFCs, even if a membrane separator is maintained between the two cell compartments. This phenomenon is accelerated under O_2 excess.[50] Various directions have been explored to resolve this issue. The first one is a reconstitution of an *in vivo*

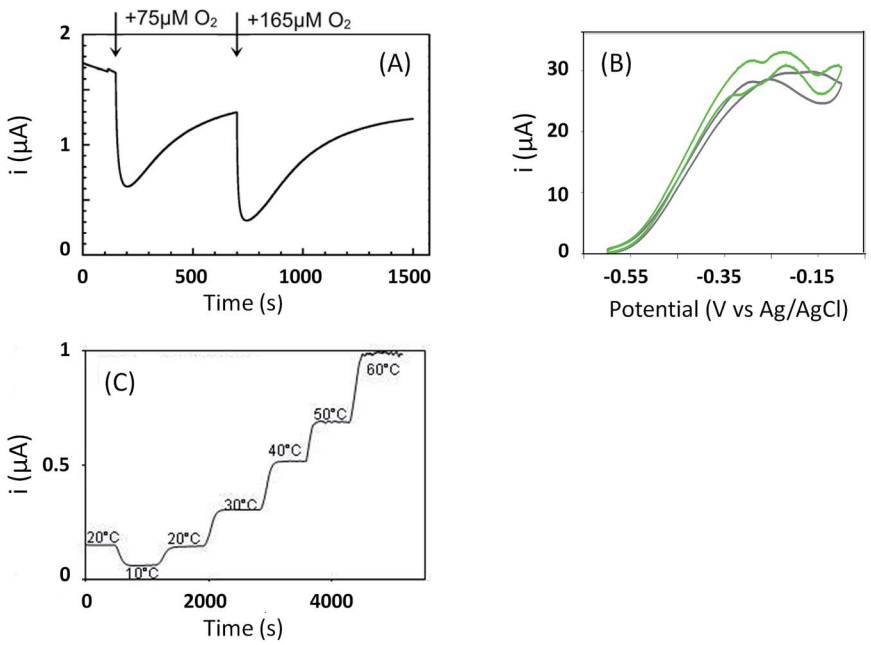

Fig. 6 The membrane-bound [NiFe]-hydrogenase from *Aquifex aeolicus* presents outstanding properties. (A) O_2-tolerance: H_2 oxidation activity is recovered after O_2 injection at $E_{applied} = 0$ V *vs.* Ag/AgCl. (B) CO-resistance: H_2 oxidation (grey curve) is unaffected by addition of CO (green curve). (C) $T°$-resistance: H_2 catalytic oxidation current is stable on the 10–60 °C temperature range. (A) is reprinted with permission from Pandelia *et al.*, *J. Am. Chem. Soc.*, 2010, **132**, 6991–7004. Copyright 2017 American Chemical Society. (C) is reprinted from Monsalve *et al.*, *ChemElectroChem*, 2016, **3**, 2179–2188. Copyright 2017 Willey.

reactivation mechanism at the electrode. We just discussed above that oligomeric forms of hydrogenase could provide the sink of electrons necessary to maintain the activity under oxidative conditions.[67] The two dimers in the tetrameric forms would be able to share electrons through the distal FeS cluster. This is supported by a crystal structure of a dimer of *Ec*Hyd1 which underlines a distance between the two distal FeS clusters of each monomer compatible with electron transfer.[71] *In vivo* like strategy was used by Wait *et al.* under EFC conditions.[51] Starting from the knowledge that an inactivated enzyme can be reactivated under reducing conditions, the idea consisted in the direct connection of a second hydrogenase-based anode to refill electrons to the deactivated anode. H_2 oxidation at the second anode provided electrons required to reactivate the first inactivated bioanode. This resulted in the EFC recovery, and constitutes one solution to address anaerobic hydrogenase inactivation at high potentials. Another strategy was proposed by Ciaccafava *et al.* who demonstrated that O_2-tolerant *Aa* MbH could be reactivated by light[72] (Fig. 7). Actually, the magnitude of photocurrents was shown to be dependent on potential, and rate of photooxidation was shown to depend upon light intensity for potentials above Ni-B formation potential. The light-induced reactivation process of *Aa* MbH under turnover was thus hypothesized to promote the loss of the hydroxyl ligand bridging the Ni and Fe atoms. Unfortunately, attachment of *Aa* MbH to quantum rods did not allow the immobilized enzyme to assess the light induced reactivation because of the requirement of a redox mediator to oxidize H_2.[73] The last strategy explored to suppress anaerobic oxidative inactivation was reported by So *et al.*[74,75] Both O_2-tolerant *Hm* MbH and the O_2-sensitive hydrogenase from *Desulfovibrio vulgaris* Miyazaki (*Dv* MF) were immobilized on gas diffusion electrodes made of Ketjen black (KB) deposited on carbon cloth. In this configuration, H_2 is supplied from the gas phase, diminishing the limitation induced by low concentrations of hydrogen in buffer solutions. Electrochemical results were analyzed by a modeling approach that considered a competition between Ni-B formation from Ni-SI and catalytic reduction of Ni-SI by H_2. While it remains unclear if H_2 concentration in the gas diffusion electrode exceeds Henry's law saturation limit, it was proposed that it was sufficient to avoid the formation of the high potential inactive state for *Hm* MbH, and to limit its formation for *Dv* MF.[74,75]

The strategies just discussed to overcome the issues of oxidative inactivation of hydrogenases are all based on DET between the enzyme and the electrode. DET is usually preferred to MET for fundamental studies because it allows to obtain kinetic data on the enzymatic catalysis. DET is also preferred nowadays to MET for biotechnological devices because of the lower overvoltage for the transformation of the substrate, and avoidance of redox mediators that are often toxic and not easily co-immobilized with enzyme on the electrode while retaining a high catalytic efficiency. MET is however the strategy used *in vivo* for electron transfer. Radu *et al.*[76] immobilized membrane fractions of *Re* MbH including cytochrome *b* and quinone pool in tethered bilayer lipid membranes on gold electrodes. In such architecture, the physiological catalytic function of *Re* MbH is restored through a true electron transfer pathway from the [NiFe] active site to the electrode *via* the quinone pool. This elegant reconstitution demonstrated that hydrogenase did not inactivate at high potentials even under conditions of low H_2 concentrations, a behavior completely different from the usual inactivation observed with purified *Re* MbH at the electrode. It was proposed that the higher oligomeric states inside the membrane prevent the Ni-B state formation by allowing one active oligomer to donate electrons, thus reactivating a neighboring inactive oligomer. However, in this configuration *Re* MbH is not placed in direct connection with the electrode, so it is difficult to determine the exact potential it is subjected to. *In vitro*, it was shown by Plumeré *et al.* that MET can be beneficial in the case of hydrogenase, because it prevents the formation of the Ni-B inactive state.[77] *Dv* MF O_2-sensitive hydrogenase was

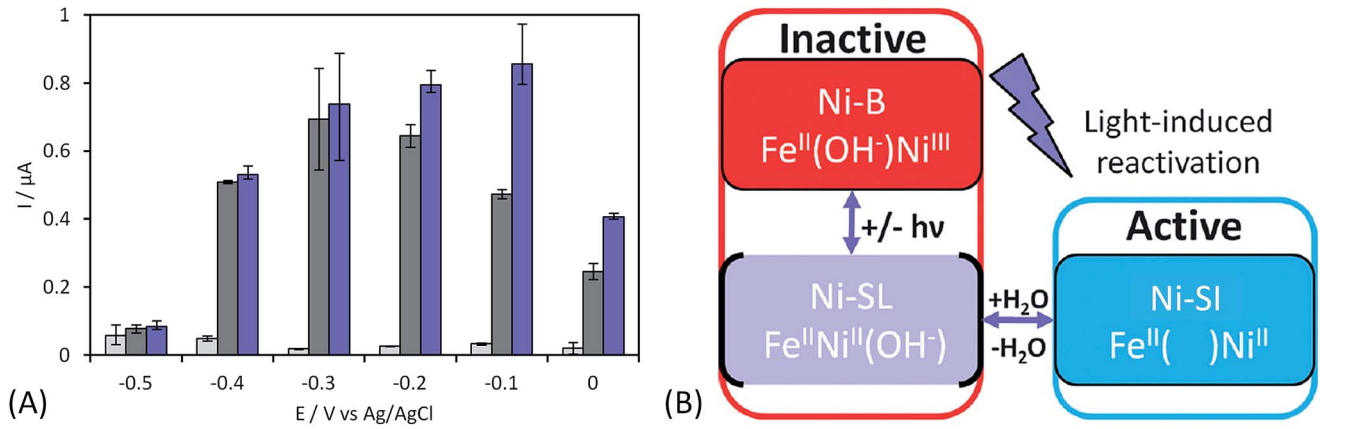

Fig. 7 Light induced reactivation of *Aa* [NiFe]-hydrogenase and proposed mechanism. (A) Catalytic current obtained for H_2 oxidation under illumination as a function of applied potential (purple columns) compared to catalytic current in the dark (grey columns) underlines that Ni-B can be reactivated by light. (B) Reactivation mechanism under irradiation is proposed to promote the loss of hydroxo ligand on the photo-induced Ni-SL intermediate from Ni-B to Ni-SI. Adapted from Ciaccafava *et al.*, *Phys. Chem. Chem. Phys.*, 2013, **39**, 16463–16467. Copyright 2017 Royal Society of Chemistry.

embedded in redox hydrogels based on viologen entities. No deactivation at high potential was observed in the cyclic voltammograms. Spectroelectrochemical Fourier transform infrared experiments confirmed the absence of Ni-B formation as MET proceeds at high potentials. This protective process is most probably linked to the fact that the enzyme experiences the redox potential of viologen, but not the potential of the electrode. It should be noted that a similar result was observed by incorporation of *Df* O_2-sensitive hydrogenase in a viologen-polypyrrole matrix some years before, although the protective role of the polymer matrix was not recognized at that time.[78] The protective role of redox hydrogels may not be effective for O_2-tolerant hydrogenases, however. Indeed, in this case higher redox potential mediators are required to fit the higher operational potentials of these hydrogenases. The potential of redox mediators may then be too high to prevent oxidative deactivation.

Use of nanomaterials to enhance the power

The enhancement of the currents delivered by the bioelectrodes is required to power real devices by EFCs. Actually, planar electrodes limit the amount of available enzymes, hence the catalytic currents. It is difficult to assess the maximum attainable current because in most cases no information on the true quantity of electroactive enzymes is available. Assuming an average turnover k_{cat} between 100 and 1000 s^{-1}, and a maximal amount of a monolayer of electrocatalytically active enzymes, current densities would be limited to around 1 mA cm^{-2}. On the contrary, the use of nanomaterials presenting a high surface/volume ratio will *a priori* increase the loading of enzymes per geometric area unit. Although many works have been reported since more than 15 years in this domain, research towards 3D architectures for both enzymatic H_2 oxidation and O_2 reduction is still very active.[3,4,79–82] The interest has moved from amplification of the catalytic current by an increase in the developed electroactive surfaces, to more fundamental queries on the relation between loading/orientation/conformation/activity of the enzyme inside the nanostructures. Both DET and MET are considered, but the issues that need to be addressed are different depending whether DET or MET process is used for the electrocatalysis. Certainly, this section will not be exhaustive because this is beyond the scope of this review, but it will give the recent main results and current open questions in the use of nanomaterials for hydrogenase and BOD bioelectrochemistry.

A variety of nanomaterials

For a DET process, the aim is to increase the amount of enzymes able to communicate directly with the electrochemical interface. Thus nanomaterials behave as ideal platforms to increase the surface area, to ensure intimate electric contact with enzymes, and potentially decrease the tunneling distance between active sites or surface electronic relays and electrode. In the particular case of EFCs, the current densities are expected to be sufficiently high to achieve useful power. Accordingly, this imposes high specific conductivity of the electrode material to avoid ohmic losses. That is why two kinds of highly conductive nanomaterials are particularly often used in EFCs: carbon and gold nanomaterials (Fig. 8).

Carbon-based nanomaterials are the most popular for bioelectrode design.[83,84] The graphene sheet is the building block of most of the carbon nanostructures. It possesses a high conductivity and an extraordinary surface area estimated to be about 2630 $m^2\ g^{-1}$.[3] It can be wrapped to form fullerenes, rolled along the axis to form nanotubes and stacked to form graphite.[85] Although it was considered as a very attractive material when discovered, the advantage of using graphene in bioelectrocatalysis has not been fully demonstrated yet.[86] This may be due to the difficulty to obtain and handle perfect monolayer graphene sheets, and from the fact that most of the studies are performed with (electro)chemically reduced graphene oxide (rGO) which still contains some oxygen functions and has different electronic properties than graphene.[84] It has never been used for hydrogenase immobilization, and very poor catalytic signals are most often observed after BOD immobilization on rGO sheets.[87] Enhanced electroenzymatic currents could be rather attributed to the deposit of carbon nanotubes (CNTs) on graphene used as a platform.[87,88] However, some recent studies tend to demonstrate the usefulness of graphene for enzymatic O_2 reduction. Catalytic current density around 0.5 mA cm^{-2} was reported for O_2 reduction by BOD integrated within rGO.[89,90] Besides, enzyme surface coverage and the rate of interfacial electron transfer were shown to depend on the density of charges on the graphene surface. This point will be discussed further in the stability section.

CNTs appear to be the nanomaterials of choice for both BOD[70,91] and hydrogenase immobilization,[53,56,57,83,92–97] thanks to their high conductivity, chemical and thermal stability.[97] CNTs can be either single-walled (SWCNTs) or multi-walled (MWCNTs). In both cases, enzymes can readily interact with them through electrostatic and van der Waals forces. The chirality and diameter of SWCNTs control their electrical conductivity, resulting in either semi-conducting or metallic materials. On the other hand, MWCNTs can only be metallic, which makes them a more attractive material for bioelectrocatalysis. Their nanometric size and curvature comparable with enzyme dimensions may also be a key point.[79] CNTs can be arranged in a multitude of different geometries (isolated tubes, planar arrays, random networks, or forests) that are currently explored for H_2 oxidation and O_2 reduction.[92,98,99] They can be compacted into disks,[100] arranged to form flexible buckypaper films with μm thickness,[101] deposited at electrode surfaces by layer-by-layer drop casting,[53,94,96] or painted as an ink.[102] Although catalytic currents are enhanced in all the cases, the respective role of increase in the electroactive surface area, in the heterogeneous electron transfer rate or in the loading of electroactive enzymes need to be elucidated.

Nano- and microfibers are other examples of carbon based nanomaterials being considered more recently, which provide a large surface area for potential attachment or entrapment of enzymes. Compared to CNTs, carbon nanofibers (CNFs) usually have smaller specific surface areas, but instead, they represent

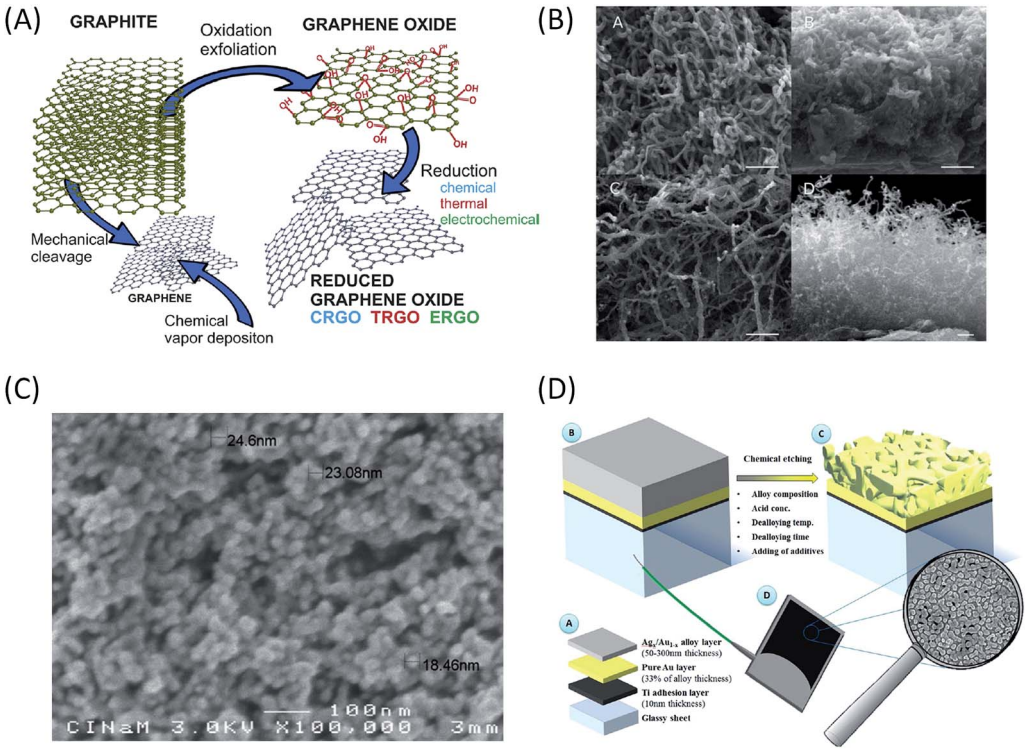

Fig. 8 A variety of nanomaterials can be used for enzyme immobilization. (A) Preparation of graphene and rGO (reproduced from Filip *et al.*, *Electrochim. Acta*, 2014, **136**, 340–354); (B) CNT forests (reproduced from Zelechowska *et al.*, *Sensors Actuators B*, 2017, **240**, 1308–1313); (C) AuNP layer-by-layer deposits (reproduced from Monsalve *et al.*, *Bioelectrochem.*, 2015, **106**, 47–55); (D) nanoporous gold electrode obtained from dealloying process (reproduced from Siepenkoetter *et al.*, *Electroanal.*, 2016, **28**, 2415–2423). Copyright 2017 Elsevier.

a bigger and more open macroporous structure thus allowing enhancement of substrate diffusion towards the immobilized enzymes. CNFs made by graphene cone stacks and coated on a PG electrode were used for *Aa* MbH immobilization. Such modification allowed a current density of 4.5 mA cm^{-2} for enzymatic H_2 oxidation, which was one of the highest current density ever reported.[103]

Upon enzyme-loading increase, substrate depletion is likely to occur. This is especially critical when talking about highly active enzymes like hydrogenases and low solubility of gaseous substrates (*e.g.* H_2 and O_2) in water-based solutions. Apart from specific EFC design such as microfluidic substrate distribution, larger pores of the carbon support are thus desirable. In general, larger pores can be obtained through carbon felts (CFs), carbon cryogels, or carbon foams which present interesting properties of mechanical strength and stability.[104–107] These macroscopic supports often have a defined geometric shape that can be easily modeled depending on the application. Furthermore, their mechanical stiffness facilitates manipulation. Large porosity in such materials, has a positive impact on the magnitude of catalytic current. However, it is difficult to relate this enhanced catalytic current to a larger amount of connected enzymes or to facilitated substrate diffusion. Different nanomaterials can be mixed to provide a hierarchical interconnected porous structure with the ability to reach a tunable pore size. Mesopores are desirable for enzyme anchorage while ensuring efficient substrate delivery in large macropores. It should be noted that micropores below 2 nm range are quasi-useless for EFC since they are too small for enzymes to penetrate and give rise to high capacitive current contribution which is usually undesirable except in some specific cases. In order to improve the favorable characteristics of porous materials, their macrostructure can thus be used as a primary framework towards 3D hierarchically structured materials by incorporation of a secondary structure of smaller dimensions like CNTs.[108] For example, CNTs were deposited on the microfibers of carbon felts for H_2 oxidation by *Aa* MbH.[109] The developed electroactive surface evaluated by capacitance measurement was 5 times higher compared to that of the bare CF. In another work, a wet-spinning approach was used to fabricate electrodes in the form of microfibers, in which CNTs and enzymes for O_2 reduction were directly imbricated.[110,111] Pore size can otherwise be tuned and controlled using templated carbons such as MgO-based ones.[112] Modeling has not been largely applied to such a system yet, but it will certainly help in the rationalization of porosity.

Gold nanoparticles (AuNPs) are another type of nanomaterials that have unique physicochemical characteristics and optical-electronic properties. They have been largely used for H_2 oxidation and O_2 reduction by enzymes. Their synthesis drives their properties, which can be tuned by changing their shapes, sizes and chemical environments. The most common preparations of AuNPs are either by physical "top-down" methods where the bulk is divided into smaller units, or by "bottom-up"

chemical methods. The latter starts with a reduction of an Au-precursor creating metal clusters followed by their aggregation into particles and growth until the desired size.[113] Despite the common acceptance that nanoparticles by themselves enhance electron transfer, a decisive study to clarify the influence of the size of nanoparticles in biocatalysis (current and reaction overpotential) was done by Pankratov *et al.*[114] The authors modified bare Au electrodes with a sub-monolayer of AuNPs. It was found that AuNPs with a size at least four times bigger than the enzyme (20–80 nm) influenced neither the direct electron transfer rate nor the overpotential of O_2 bioelectrocatalysis compared to bare Au electrodes. Similar results were obtained by immobilizing *Aa* MbH on AuNPs of two different sizes.[106] In this latter study, multilayers of AuNPs were deposited on a gold electrode showing increasing catalytic currents for H_2 oxidation up to 1.8 mA cm^{-2}, *i.e.* 150 times more than the current recorded on the bare gold electrode. However, when reported to the real developed electroactive area, which can easily be deduced from simple cyclic voltammetry experiments in acidic solution, it was demonstrated that the enhancement in catalytic current was simply correlated to the surface area increase.

Other nanostructured materials are worth mentioning. Co-deposition of different nanomaterials is explored, such as AuNPs and CNTs deposited onto electrospun polyacrylonitrile microfibers.[88] Nano- or mesoporous gold electrodes are promising materials. They were used to enhance DET with *Mv* BOD.[115] As the diameter of the pores is expected to play a key role in the loading of electroactive enzymes, the pore size of the nanoporous gold electrode was varied between 4 and 78 nm thanks to Au/Ag dealloying processes at different temperatures.[116] The catalytic current was shown to be the highest for a pore size of 8 nm, *i.e.* slightly higher than the BOD size. For higher pore dimension the current decreased. The authors concluded that BOD did not diffuse deeply inside the electrode, and that catalysis occurred mainly on the surface of the nanoporous electrode. The results can however suggest that 8 nm is the most suitable pore size for hosting a single enzyme molecule, thus favoring an excellent electrical connection.

Enzyme distribution in mesoporous and nanomaterials

There is a general assumption that enzymes are homogenously distributed throughout the entire nanomaterial volume with an optimal microenvironment to favor catalytic activity. Nonetheless, enzyme distribution should not only depend on the material properties, but also on the interactions the enzyme is subjected to during the immobilization process, and on the immobilization process itself. The correlation between enzyme distribution and electrochemical response is thus important to gather fundamental knowledge about substrate/enzyme diffusion restrictions that can compromise performance. This is also a prerequisite to optimize the loading of the electroactive enzyme. Indeed, even when enzymes are compacted with carbon particles into free-standing pellets, the intimate mixture does not preclude aggregates of inactive enzymes to be formed. This is especially true because large amounts of enzymes are generally used in this configuration.[100] One relevant demonstration of non-homogeneous enzyme distribution in the porous matrix was given by the results obtained using fluorescence confocal microscopy to follow the distribution of malate dehydrogenase immobilized in macroporous chitosan. The images suggested that enzyme distribution was dependent on the interactions between the biomolecules and the charged polymer species that create a singular chemical microenvironment.[117] Few studies however address such issues with hydrogenases and BODs. Complementary to electrochemistry measurements of O_2 reduction using wet-spun carbon fibers directly fabricated with BOD and CNTs inside the fibers, Mateo–Mateo *et al.* corroborated the presence of *Magnaporthe oryzae* BOD within a fiber by confocal fluorescence microscopy experiments and transmission electron microscopy with EDX analysis of the cross section of CNT fibers. The images and EDX indicated the presence of BOD throughout the fiber, from its outer surface to its core[110] (Fig. 9).

The embedding of enzymes and CNTs in the core fiber was shown to favor DET. However, these images show the total enzyme distribution and do not allow the deduction of the fraction of them participating actually in the biocatalysis. Armstrong *et al.* compared the electrocatalytic activity of *Ec*Hyd1 in a cylinder or in a half cylinder of compacted graphite particles. The twice less catalytic current in the half cylinder suggested a homogeneous distribution of enzymes inside the entire porous matrix.[118] Nevertheless, the very few data on enzyme distribution in a porous matrix imposes development of tools to couple electrochemistry to surface imaging and other techniques to realize enzyme cartography of various bioelectrodes.

From enzyme orientation on planar electrodes…

As mentioned earlier, the large size of enzyme molecules and active sites buried within the protein shell often require the molecule to be adsorbed in specific orientations to perform electron transfer. It results in a low amount of electroactive enzyme molecules among adsorbed ones, and the appearance of a linear region on DET voltammograms due to the dispersion of enzyme orientations.[119,120] From the practical point of view, the dispersion of orientations should be minimized and enzyme should be immobilized in a defined orientation bringing the surface electron relay as close as possible to the electrode surface in order to maximize the current densities. This can be done by rational electrode modification.

In vivo, the orientation of an enzyme in a metabolic chain before electron transfer is most often driven by electrostatic interactions between interacting partners.[121] Transitory complexes are formed which put the interacting redox sites at a minimal distance to optimize the electron transfer rate. This molecular recognition can serve as a model for chemical modification of electrochemical interfaces suitable for enzyme orientation. If the electron transfer chain is unknown, the examination of the secondary structure of the enzyme may help in the definition of the key amino acids for proper orientation. Hence, self-assembled-monolayers (SAM) on gold can be used

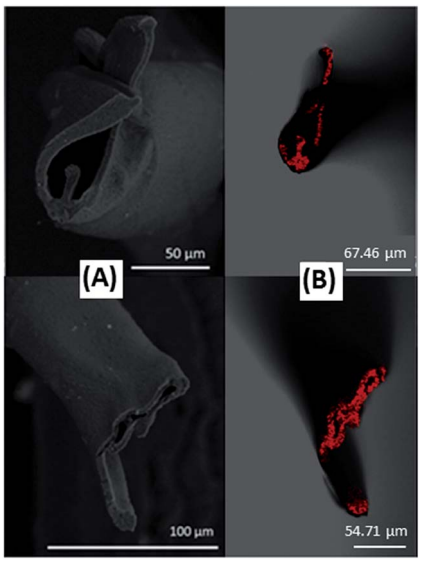

Fig. 9 (A) Scanning electron microscopy cross-sectional images of a spun CNT/enzyme fiber. Top and down are two images of the same fiber. (B) Superposition of (A) and of the images obtained using confocal fluorescence microscopy of the same cross sections with BOD labeled with a fluorescent dye. Adapted from Mateo–Mateo *et al.*, *ChemElectroChem.*, 2015, **2**, 1908–1912. Copyright 2017 Willey.

to tune the chemical functions of the electrode in order to recognize the target residues. Let us consider the examples of *Aa* MbH and *Mv* BOD to illustrate the orientation issue on planar electrodes.

In the case of hydrogenase, the exit point of electrons consecutive to H_2 oxidation is the distal FeS cluster. In our group, we examined the oriented immobilization of *Aa* MbH on SAM by electrochemistry and polarization modulated infrared reflection absorption spectroscopy (PMIRRAS).[122] Briefly, H_2 oxidation mainly proceeded through MET on hydrophobic SAMs, while both DET and MET were observed on hydrophilic SAMs (neutral, positive or negative). The two different electrochemical processes according to the SAM hydrophobicity were proved to be correlated to different orientations of the enzyme. Absence of DET on hydrophobic surfaces was explained by the presence of surfactant surrounding the trans-membrane helix. This helix is less than 15 Å from the FeS distal, thus defining a hydrophilic domain pushing away the exit point of electrons.[123] Coexistence of DET and MET was attributed to a distribution of orientation: some enzymes are positioned at the electrode with the distal FeS cluster at a tunneling distance from the electrode surface, compatible with DET, and others are placed with the distal FeS cluster far from the electrode, thus requiring a redox mediator for electrocatalysis. This absence of enzyme orientation by electrostatic interactions is linked to the membrane position of the enzyme, which uses the hydrophobic trans-membrane helix for membrane anchorage with no intervention of electrostatic interactions. Molecular dynamics (MD) confirmed this assumption, underlining a low dipole moment whose direction fluctuates largely.[124] MD analysis further underlined that orientations for DET should be preferred on positive interfaces (Fig. 10). Similar conclusions were drawn by Heidary *et al.* for *Re* MbH.[125]

A different scheme can be drawn for *Mv* BOD immobilization on SAMs. *Mv* BOD is a nice model, because its crystallographic structure has been resolved.[126] The entry point of electrons is the T1 Cu. *Mv* BOD structure displays a dipole moment of 752 Debye pointing toward a highly positive patch formed by 4 arginine ($pK_a = 12.5$) residues surrounding the T1 Cu center. Such an environment is expected to promote DET by electrostatic interactions on negatively charged interfaces. Accordingly, only the DET process was recorded for O_2 reduction with *Mv* BOD immobilized on negatively charged SAMs, and only the MET process on positively charged SAMs, suggesting a specific orientation according to favorable electrostatic interactions.[127,128]

…to enzyme orientation in mesoporous structures and on nanomaterials

Turning back to one fundamental question: can nanostructuration help overcome the orientation limitation? If not, can the molecular determinants for enzyme orientation obtained on planar electrodes be extended to macroporous, meso-, and nanomaterials?

The pore size effect on bioelectrocatalysis was recently modelled by Sugimoto *et al.*[129] in the case of *Mv* BOD and *Dv* MF hydrogenase immobilized in mesoporous KB material. The authors concluded that an enzyme molecule encapsulated in pores of comparable size has a higher probability to be in electric connection whatever its orientation.[129] On the other hand, for pore size much larger than enzyme dimensions, macroporous and planar electrodes gave similar electrochemical signals. The difference becomes more pronounced with bigger enzyme molecules. These findings have major consequences on the use of porous materials for bioelectrocatalysis, at least if one wants to take benefit from the porosity.

Quinson *et al.* compared various carbon-based materials (micron-sized graphite particles, CNTs, nanofibers and carbon blacks) showing different morphologies, graphitic structures and specific surface areas.[83] Comparative H_2 oxidation by immobilized *Ec*Hyd1 led to the main conclusion that there was no strong difference in the distribution of orientations of the enzyme as a function of the carbon type. In the case of the carbon blacks, this was explained by the size of the pores which was determined to be in the range 3.5–9 nm within all the carbon materials, *i.e.* in the same range than the enzyme, thus favoring the electrical contact with hydrogenase. In the particular case of CNTs, accurate comparison was not realized in this study. However, when enzymes are immobilized on CNTs either arranged within films or part of macro- or mesoporous structures, hierarchical porosity may induce heterogeneity of enzyme orientation. Hence, the demonstration of orientation distribution, and the tools to control efficient orientation is certainly the most important breakthrough in the domain for the last two years.

Monsalve *et al.*[57] considered H_2 oxidation by *Aa* MbH immobilized on different CNT surfaces. Not only can CNTs develop large surface areas, but their walls can be chemically

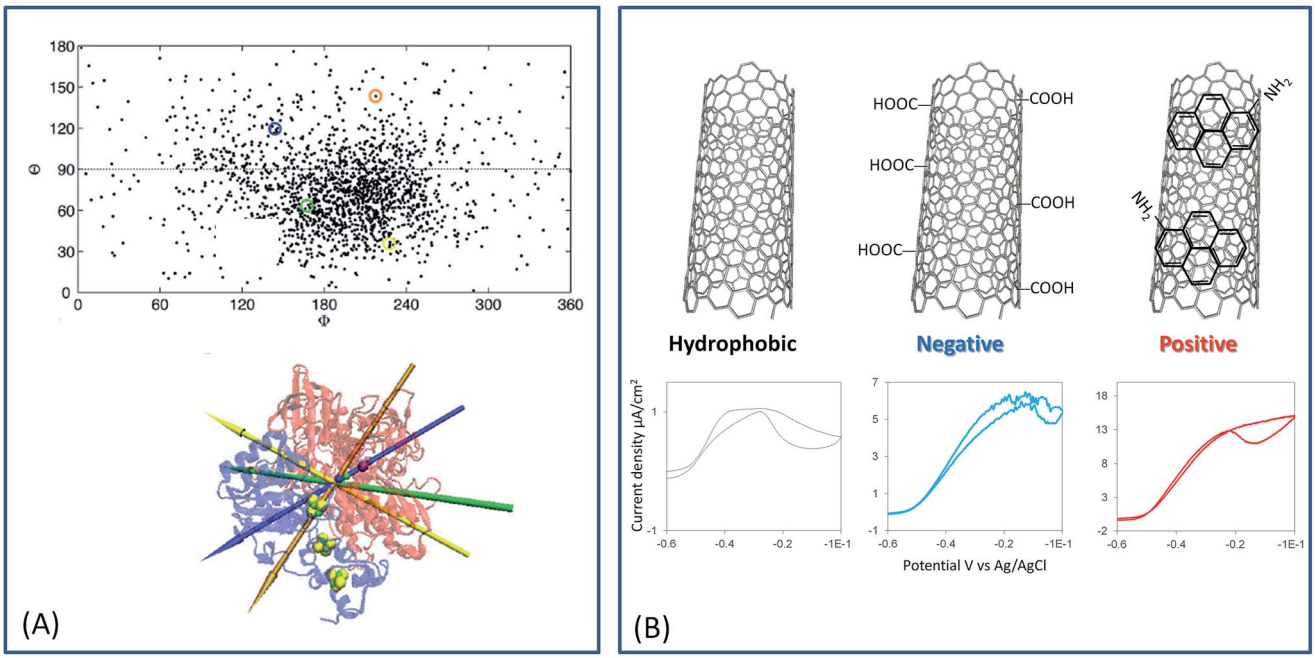

Fig. 10 Orientation of dipole moment and large dipole moment fluctuation of *Aa* MbH obtained from MD (A) suggest a favored orientation for DET on positively charged interfaces, which is assessed by H_2 oxidation by the enzyme immobilized on CNTs with different functionalities (B). (A) is adapted from Oteri *et al.*, *Phys. Chem. Chem. Phys.*, 2014, **16**, 11318–11322. Copyright 2017 Royal Society of Chemistry. (B) is adapted from Monsalve *et al.*, *ChemElectroChem.*, 2016, **3**, 2179–2188. Copyright 2017 Willey.

modified by oxidative treatment, by π–π stacking of poly-aromatic derivatives or by reduction of diazonium salts.[84] Thus, they behave as versatile platforms for studying enzyme oriented immobilization. In the case of *Aa* MbH, three different CNT surfaces were studied, *i.e.* hydrophobic pristine CNTs, carboxylic- and amino-functionalized CNTs (renamed COOHCNT and NH_2CNT respectively). The carboxylic functions were generated by oxidative treatment of CNTs, while amino ones were formed by π–π stacking of aminomethyl-pyrene, inducing negative and positive charges on the CNT walls at neutral pH, respectively. Films of the various CNTs were made by successive drop castings on a PG electrode. The surface area of the modified electrode was estimated from the capacitive current at a potential where faradic processes are minimal, and the catalytic currents were reported to the real electroactive surface area. In that way the catalytic current densities depend on the quantity of enzymes orientated favorably for DET on the CNTs. Only the hydrophilic CNT films, *i.e.* COOHCNTs or NH_2CNTs, gave rise to enhanced catalytic current densities compared to the bare PG electrode. More interestingly, catalytic current density on the positively charged NH_2CNTs was at least twice higher than that recorded on negatively charged COOHCNTs. These results provided experimental proof of a better orientation for DET of *Aa* MbH on positive interfaces, and underlined a full agreement with the model proposed on SAMs and confirmed by MD (Fig. 10).

Contrary to *Aa* MbH, many studies based on *Mv* BOD are available to assess the validity of molecular determinants determined on planar electrodes for porous ones. As the first answer, dos Santos *et al.* modified a PG electrode with different aromatic compounds, bearing amino or carboxyl groups,[40] and studied enzymatic O_2 reduction by coated *Mv* BOD. The roughness of the PG surface is sufficient to consider this electrode as non-planar albeit it cannot be considered as a true porous electrode. It was demonstrated that only modifiers containing carboxylates showed enhanced catalytic currents compared to bare PG electrode. This result is in agreement with data on SAMs. The use of aromatic compounds can furthermore play a role by mimicking the natural substrates of BOD.[130] Unfortunately, in case of amino derivatives, the MET process was not evaluated, precluding the evaluation of the percentage of well oriented enzymes. Electrodeposited reduced graphene oxide was used as a platform for *Mv* BOD immobilization.[89] High porosity was shown with macropores in the range of 10–20 μm within rGO aggregates. rGO was functionalized by diazonium salt reduction to provide naphtoic acid functionalities on the surface. DET for O_2 reduction by *Mv* BOD was observed, although the addition of ABTS as a redox mediator gave rise to MET currents. This result would suggest a distribution of orientation of the enzyme on the surface. However, the immobilization was made in the presence of a coupling agent which can favor immobilization of enzymes in various orientations.

More insights into *Mv* BOD orientation in the porous matrix was gained by the use of CNT films. Bilirubin, the natural substrate of *Mv* BOD, as well as its functional analogues, was used to modify CNTs. With the DET/(DET + MET) ratio more than 90%, enhanced catalytic currents were attributed to the proper orientation of BOD.[131,132] The strategy was extended by Lalaoui *et al.* by use of porphyrin-functionalized CNTs.[91] The idea was to promote proper BOD orientation by use of bilirubin

precursors. A non-catalytic pH-dependent signal attributed to T1 Cu was observed allowing us to propose the involvement of histidine residue in the electron transfer process. A kinetic model was used to fit the catalytic cyclic voltammograms.[120] It was demonstrated that protoporphyrin IX, the closest to the bilirubin structure, enabled proper BOD orientation. At the same time, protoporphyrin derivatives deprived of ionisable carboxylic moieties resulted in much worse orientation arguing again for the importance of negative charge. Given the catalytic current and the coverage of electroactive BOD, a high value of $k_{cat} = 2400\ s^{-1}$ was calculated. However, there is still some doubt whether the non-catalytic signals are related to enzymes effectively participating in catalysis. The same group reported the effect of the nature of chemical functions carried by CNTs on the electrocatalysis by *Mv* BOD.[133,134] While on the negatively charged CNTs, DET occurred at the T1 Cu centre, O_2 reduction was shown to occur at much lower potentials on positively charged CNTs. The latter catalytic process was attributed to a catalytic pathway through a partially oxidized form of the TNC, previously identified in the presence of chloride.[135]

Mazurenko *et al.* studied in depth the influence of the chemistry of CNTs on the O_2 catalytic reduction by *Mv* BOD using an integrative approach that considers both the enzyme and the electrode surface[70] (Fig. 11). Hydrophobic pristine CNTs, COOHCNTs and NH2CNTs were compared. Careful determination of the chemical composition and charge carried by each type of CNTs was made by XPS, and zeta potential was measured as a function of pH. The adsorption of *Mv* BOD was realized at different pH values in the range of pH 3–8, and the catalytic process for O_2 reduction was quantified by electrochemistry and modelling before and after ABTS addition. The study also included the evolution of charges and dipole moments of the enzyme as a function of pH. This strategy allowed to provide a rational understanding of BOD/CNTs interactions. On NH_2CNTs, MET/DET ratio increased with decreasing pHs, in relation with progressive appearance of positive charges on CNTs. However, no catalytic wave attributed to an electron pathway through the TNC was observed as stated in the former work by Lalaoui *et al.* The origin of the discrepancy is not clear yet. It was confirmed that carboxylic functions favor DET and narrow BOD distribution orientation, except at very low pH < 4 where the carboxylic functions are protonated. Similar results were obtained for BOD activity in carbon felts post-functionalized by COOHCNTs.[109,136] It is noteworthy that the density of carboxylic functions can be also modulated by the length of CNTs, hence directly influencing O_2 catalytic reduction by *Mv* BOD, with the maximum current obtained for the shortest CNTs, *i.e.* those bearing more negative charges.[137]

In parallel with *Mv* BOD, a thermostable *Bp* BOD was studied by Mazurenko *et al.*[70] The crystal structure of this BOD is not resolved yet, but a model was constructed based on its sequence. From this model, a high dipole moment associated with a negative charge in a 15 Å sphere around the T1 Cu was determined in the pH range of 4–12. This configuration is totally different from that on *Mv* BOD, suggesting also a very different catalytic behavior when immobilized on CNTs. As expected from this structural consideration, no DET was obtained on negatively charged CNTs, while a high MET current was measured. Conversely, the ratio MET/DET was close to zero in the pH range of 3–8 used for *Bp* BOD adsorption (Fig. 11). DET was however also obtained on surfaces presenting weak total charges, as in the case of pristine CNTs or CNFs.[103] These last results were attributed to nonpolar residues in the vicinity of T1 Cu.

KB electrodes were chemically modified to favor *Mv* BOD orientation towards efficient DET for O_2 reduction. As obtained with CNTs, bilirubin coating was shown to enhance the catalytic current.[138,139] A kinetic analysis of the DET signal led to the conclusion that almost all electroactive BODs adsorb in a proper orientation with some contribution of molecules in other orientations. In another report by the same group, several aromatic amines bearing various end-functions were linked to KB.[140] The highest catalytic current was obtained with carboxylate end-function compared to $-COOCH_3$ or $-NH_3^+$, with poor response in the case of $-NH_3^+$, again in agreement with the statement made on planar electrodes that negative functions promote DET on *Mv* BOD while positive ones prevent DET.

In conclusion, it appears that unless nanomaterials in which each enzyme molecule enters a pore of similar diameter to enzyme diameter are designed, surface chemical modification is required for enzyme orientation yielding efficient catalysis in porous electrodes. This general rule has been verified with other enzymes useful for H_2/O_2 EFCs. The immobilization of *Df* hydrogenase on amino-modified CNTs is fully consistent with a structure of the enzyme showing high value of dipole moment and a strong acidic patch of glutamate residues around the distal FeS.[94,141] The case of *Re* MbH is more astonishing. *Re* and *Aa* MbHs share more than 60% of homology. Nevertheless, catalytic activity with *Re* MbH sharply dropped down to zero as the quantity of negative charges on the CNT surface increased.[57] This unexpected result might be explained by *Re* MbH denaturation induced by strong negative electrode charge in the absence of detergent in the enzyme solution, contrary to *Aa* MbH. Further conformational studies of enzymes immobilized on strongly charged interfaces are required in the near future.

Generally speaking, rational functionalization of mesoporous and nanomaterials with a large developed surface had drastic consequences on the enhancement of enzymatic current densities. In many cases, the current densities reported for the projected surface area of the electrodes are nowadays close to 10 mA cm^{-2}.

Case of MET in mesoporous and nanomaterials

The problem is somehow different when speaking about MET in mesoporous materials. In this case, enzymes in any orientations can *a priori* communicate with the electrode *via* the diffusing redox mediators or through electron hopping between the immobilized redox entities. Any conductive materials that can increase the loading of enzymes, while maintaining its activity and allowing substrate diffusion, should thus be suitable. In the particular case of redox polymers such as widely used redox hydrogels, the polymer itself can be made thick enough to incorporate a large amount of enzymes, although with very

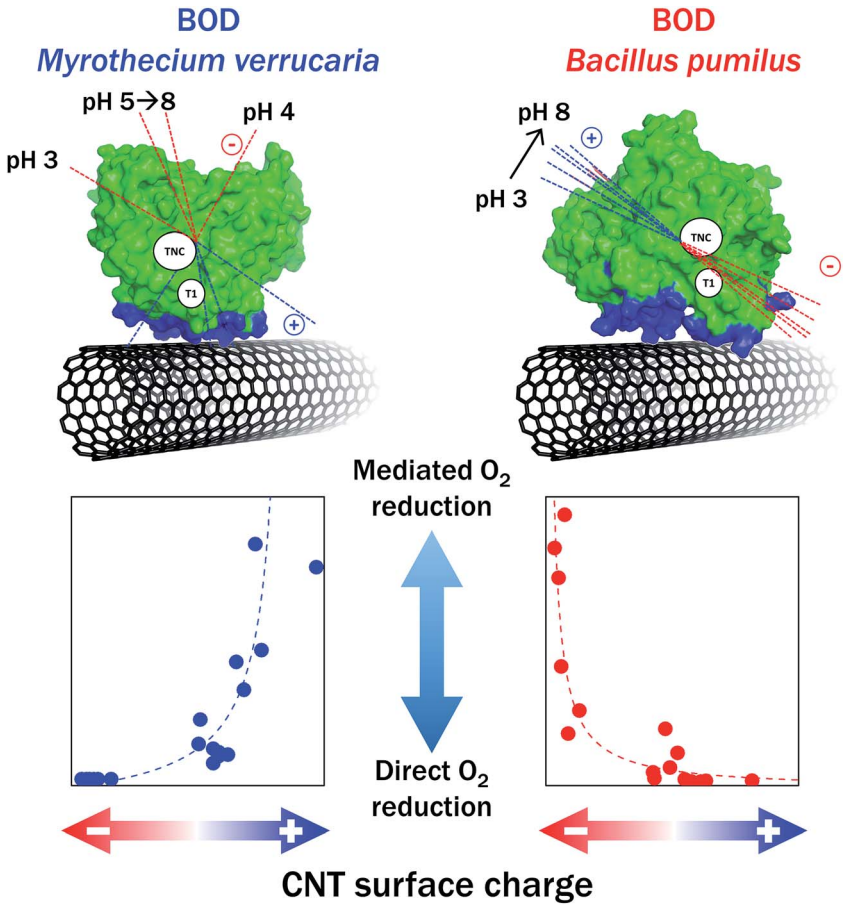

Fig. 11 Electrostatic interactions between *Mv* and *Bp* BODs and CNTs bearing various charges control the DET or MET processes for O_2 reduction. Adapted from Mazurenko *et al. ACS Appl. Mater. Interfaces*, 2016, **8**, 23074–23085. Copyright 2017 American Chemical Society.

thick layers the entire film thickness does not take part in catalysis. Nevertheless, to further increase the currents, there is an advantage to deposit the hydrogel on porous materials as it was highlighted recently for photosystem II immobilized in the redox hydrogels on hierarchical indium tin oxide.[142] Some other relevant examples are reported in the literature. CNT polyelectrolytes with viologen substituents acting as redox mediators were synthesized and reacted with *Thiocapsa roseopersicina* hydrogenase.[143] It was proposed that CNTs act as nanoscale backbones with an increased surface area, and as electric wires for both redox mediator and hydrogenase. Oxidized CNTs were mixed with an Os-based redox polymer for *Mv* BOD encapsulation.[144] Enhanced O_2 reduction was shown to come from electron transfer through the conductive CNT networks which may assist the hopping process between the osmium entities. One main issue should be to determine the suitable pore size for the porous volume to be accessible. This is well illustrated in a very recent study dedicated to the electroactivity of enzyme embedded in an osmium polymer film deposited on/in nanoporous gold.[145] Looking at the enzymatic current as a function of pore size in the range of 10–50 nm, it clearly appears that the polymer/enzyme biocomposite was unable to fully enter the pore structure.

Bioelectrode stability: many origins, various solutions

The existence of living organisms relies on the constant renewal of enzymes,[146] so that, *in vivo*, enzymes are functioning only during limited duration.[37] It is thus expected that the stability of enzymatic electrodes is a key parameter that restricts EFCs to short term applications. As stated at the beginning of this review, screening biodiversity is the first answer for the discovery of new enzymes able to operate and be stable in various environments, including extreme ones. Otherwise, the stabilization of enzymes by immobilization on solid supports such as electrodes is still an open question. Sensitive tools are required to address this issue, and to be able to discriminate between the different origins of instability of bioelectrodes. Any variation in catalytic current needs to be attributed to higher/lower enzyme amount or more/less active enzyme, which can be itself related to enzyme reorientation, or reconformation, or denaturation. Some recent studies report the use of electrochemistry coupled to quartz crystal microbalance (e-QCM),[147,148] or surface plasmon resonance (e-SPR)[127] to determine the factors explaining the decrease in catalytic currents with time. It was established that this decrease is not related to enzyme

release from the electrode. Enhanced stability by covalent attachment of the enzyme was then attributed to rigidification of the enzyme structure. Ellipsometry,[114] PMIRRAS[127] and interferometry[148] suggested conformational changes in the enzyme structure upon immobilization. The influence of the applied potential, the drastic role of the negative charges used to properly orient the enzyme, and the influence of full enzyme coverage on the catalytic activity were also underlined. These studies have been limited to gold planar electrodes, so far. By modification of the negative charge density of reduced graphene oxide, it was nevertheless shown that the highest *Mv* BOD coverage was reached with the highest charge density while the highest heterogeneous ET was obtained with the lower charge density.[91] This result may also reflect the negative effect of the charges used for enzyme orientation on its conformational stability.

Otherwise, one of the main sources of instability in H_2/O_2 EFCs is the inhibition of hydrogenases by O_2. All the [NiFe]-hydrogenases are inactivated under O_2, but various states are formed with different reactivation rates according to the hydrogenase type. While the O_2-tolerant hydrogenases such as *Aa* MbH are able to oxidize H_2 in the presence of O_2, this is not the case for O_2-sensitive hydrogenases which require application of very low redox potentials to be reactivated. O_2 inhibition of hydrogenases thus restricts the panel of enzymes suitable as anode catalysts in H_2/O_2 EFCs.

Three main directions have been proposed to overcome aerobic inactivation of hydrogenases. The first one takes profit of the porous matrix which may be used as an electrochemical barrier to O_2. Xu *et al.* compacted CNTs alone or mixed with graphite (G/CNT) to design 0.3 mm thick disk electrodes.[149] These electrodes contain pores with diameters in the 10–70 nm range, for which effusion of H_2 occurs 4 times faster than O_2 in the gaseous phase. Thanks to this property, the porous matrix seems to act as an O_2 filter, and hydrogenases deeply embedded in the compact film become protected. Full activity of O_2-tolerant *Ec*Hyd1 in 78% H_2/22% air mixtures was thus observed. More importantly, it was demonstrated that even the O_2-sensitive [NiFe]-hydrogenase from *E. coli* (Hyd2) was able to oxidize H_2 in the presence of air. The larger the volume of mesopores, the more efficient the protection was. Depending however on the functionalities carried by CNTs, O_2 reduction can be enhanced. This is the case of CNTs modified by π–π stacking of amino-pyrene derivatives on which enhanced O_2 reduction most probably leads to reactive oxygen species (ROS). ROS were shown to be more deleterious than O_2 for *Aa* MbH, thus imposing their trapping in the outer layers of the porous matrix.[57] A second way of protection of hydrogenases against O_2 is to design the EFC itself to restrict O_2 diffusion to the anode. This is typically what is done within air-breathing hydrogen EFCs, in which O_2 is supplied from the gaseous phase.[140,150]

We have focused our review on DET processes because they are mainly used in EFCs to avoid the drawbacks linked to redox mediators already discussed above (higher overpotentials, limited kinetics, co-immobilization, toxicity, *etc.*). Nevertheless, MET has long been and is still nowadays being used in many laboratories, either to study and take benefit of the specific interactions between enzymes and their natural partners – the case of soluble O_2-sensitive hydrogenases and polyheme cytochrome c_3 is particularly relevant[151]-or to overcome the difficulties related to enzyme orientation. Redox hydrogels based on osmium redox entities were in that way very popular to embed BODs.[152,153] Whether the enzyme is more stable in such polymers compared to direct connection has not been discussed as far as we know. Hydrogenases were also previously incorporated in polymer films such as thin viologen films[78,154] or phenothiazine-based polymers.[155] Ciaccafava *et al.* suggested that the phenothiazine entity should play several roles and act as a mediator but also as a ROS scavenger to help *Aa* MbH to sustain hydrogen oxidation in the presence of oxygen. Morozov *et al.* showed O_2 tolerance of the O_2-sensitive hydrogenase from *Thiocapsa roseopersicina* when embedded in the viologen-based polymer.[154] Viologen-based protection of O_2-sensitive hydrogenases was recently rationalized by Plumeré *et al.*[77,156–158] It was demonstrated that hydrogen oxidation induced catalytic O_2 reduction by the reduced viologen entities at the polymer/solution interface. As a consequence, the bioanode displayed a half-life as high as 46 days. However, it also pointed out that, due to diffusional limitations, only a small fraction of the immobilized enzyme actually participates in the catalysis. ROS production in the film may be also questionable. As an alternative, an integral hydrogenase membrane complex might be used as a biocatalyst for H_2 oxidation. As an illustration, Radu *et al.* studied quinone mediated H_2 oxidation by the full heterotrimeric membrane-bound hydrogenase from *Re*, reconstituted on gold electrodes modified by tethered bilayer lipid membranes.[76,159] In the presence of exogenous quinones, the oligomeric state of the enzyme was shown to accelerate enzyme reactivation after O_2 addition. However, H_2 oxidation occurs at high potential, determined by that of the quinone pool, with a very low current.

The new generation of H_2/O_2 enzymatic fuel cells

Progressive advancements in nano- mesoporous matrixes suitable for enzyme incorporation, and the understanding of how enzyme orientation proceeds in such environments, have led to progressive net improvements of H_2/O_2 EFCs. Table 1 summarizes all the reported EFCs since the proof-of-concept. It clearly appears that this is still an emergent device. For comparison, in the same period several hundreds of publications reported glucose/O_2 EFCs.

A first step was jumped in 2012 in F. Armstrong's laboratory in UK, and in our group. This step was followed by improvements of the bioelectrodes in the two laboratories during the next 4 years, to finally reach a useful power level. Initially, O_2-tolerant hydrogenases and *Mv* BOD were immobilized on functionalized CNTs allowing great enhancement of the direct catalytic currents compared to bare PG. Covalent attachment between the carboxylic functions on CNTs and the enzymes improved the stability of the bioelectrodes. The design of the EFCs was however notably different in the two laboratories.

Table 1 H_2/O_2 biofuel cells from the proof of concept to powered devices

Date	Bioanode	Biocathode	Conditions	Substrate	Membrane	Power density, mW cm^{-2}	OCV, V	Stability	Ref.
2001	*Dv*H cells on CF MET by MeV in solution	*Mv* BOD on CF MET by ABTS		100% H_2–100% O_2	Yes	0.4	1.17	2 h	13
2005	*Re* MbH on PG	*Tv* LAC on PG		H_2/air	No	0.007	0.97	nd	48
2006	*Rm* CH34 MbH on PG	*Tv* LAC on PG		3% H_2 in air	No	0.005	0.950	nd	49
2010	*E. coli* Hyd1 on PG	*Mv* BOD on PG modified by 6-amino-2-naphtoïc acid		(A) 100% H_2–100% O_2 (B) 96% H_2–4% O_2 (C) 4% H_2 in air	(A) Yes, (B) and (C) No	(A) 0.063, (B) 0.013, (C) 0.010	(A) 0.99, (B) 0.95, (C) 0.93	nd	51
2012	*E. coli* Hyd1 covalently attached to MWCNT modified with butyric acid pyrene	*Mv* BOD covalently attached to MWCNT modified with butyric acid pyrene		H_2/air 80/20 mixture	No	0.119	≈1	40% loss of power after 24 h at 0.98 V	95
2012	*Aa* MbH covalently attached to SWCNT-COOH	*Mv* BOD covalently attached to SWCNT-COOH	Anode: 60 °C. Cathode: 25 °C	100% H_2–100% O_2	Yes	0.300	1.1	40% loss of power after 24 h at 0.65 V	53
2013	*E. coli* Hyd1 in compacted mesoporous carbon	*Mv* BOD in compacted mesoporous carbon	Cathode/anode surface area = 3	78% H_2–22% air	No	1.67 (reported to the anode area)	1.068	10% loss after 24 h at 0.8 V. 50% loss after one week	118
2014	*Aa* MbH in CNF	*Bp* BOD in CNF	Temperature range from 30 to 80 °C	100% H_2–100% O_2	Yes	1.5 at 60 °C	1.06	40% after 24 h at 0.5 V and 60 °C	160
2014	*Dv* MF in MeV hydrogel	*Mv* BOD covalently linked to carbon cloth	Cathode/anode surface area = 72	95% H_2–5% O_2	No	0.178	0.947		77
2014	*Citrobacter* sp. S-77 in carbon black	Pt (gas diffusion electrode)	PEMFC MEA, 60 °C		Membrane electrode assembly	180	0.95	nd	161
2015	*Aa* MbH covalent attachment on AuNP	*Mv* BOD on AuNP	Anode: 60 °C. Cathode: 25 °C	100% H_2–100% O_2	Yes	0.25	1.08	nd	106
2015	*Cr*HydA1 [FeFe]-hase in MeV-based hydrogels	*Mv* BOD on carbon cloth	Cathode/anode surface area = 200	95% H_2–5% O_2	No	0.225 (reported to anode area)	1.08	nd	157
2015	*E. coli* Hyd1 in mixtures of MWCNT and compacted graphite	*Mv* BOD in mixtures of MWCNT and compacted graphite	Cathode/anode surface area = 5	78% H_2–22% O_2	No	8 mW for 2[4 × 4] multi-cell	2.09	No decrease in the intensity of a powered LED for 8 h	149
2015	*Aa* MbH in CF modified by SWCNT-COOH	*Mv* BOD in CF modified by SWCNT-COOH	Anode: 60 °C. Cathode: 25 °C	100% H_2–100% O_2	Yes	410 μW	1.12	Data sent wirelessly every 25 s during 7 h	109
2015	*Aa* MbH on naphtoic-modified MWCNT	*Bp* BOD on pristine MWCNT	Air-breathing cathode	100% H_2	No	0.72 at 40 °C	0.95	nd	150

Table 1 (*Contd.*)

Date	Bioanode	Biocathode	Conditions	Substrate	Membrane	Power density, mW cm^{-2}	OCV, V	Stability	Ref.
2016	*E. coli* hyd1 in MWCNT	*Mv* BOD in MWCNT	Ionic liquid electrolyte	96% H_2–4% O_2	No	0.007	0.86	Stability for 9 h	162
2016	*Dv* Miyazaki MbH in Ketjen black modified with phenylenediamine	*Mv* BOD in Ketjen black modified with aminobenzoic acid	Gas diffusion system	H_2/air	No	6.1	1.12	nd	140
2016	*Aa* MbH on Pyrene-NH_2 modified MWCNT	*Mv* BOD on MWCNT-COOH		15% H_2–85% O_2	No	0.07	0.95	nd	57
2016	*Dv* Miyazaki MbH in Ketjen black	*Mv* BOD in Ketjen black modified bilirubin	Gas diffusion system	H_2/air	No	8.4 (calculated from the half cells)	1.14	nd	163

The EFC from Armstrong's group used *Ec*Hyd1 as anodic enzyme.[95] No membrane was used to separate the two compartments and the EFC was fed with a 80/20 H_2/air mixture. The average power density was 119 μW cm^{-2}. The stability of the EFC was studied at a potential of 0.98 V. 40% loss was observed after 24 h of continuous operation. Fuel and oxidant supply was shown to limit the process. A gas bubbler was also required to be close to the cathode to compensate for the low oxygen availability. One year later, these last issues were partially overcome by using compacted mesoporous carbon in which enzymes were simply incorporated, and by varying the respective dimensions of the anode and cathode.[117] Based on the total loading of enzyme, apparent TOFs of 6 s^{-1} and 0.4 s^{-1} were calculated for *Ec*Hyd1 and *Mv* BOD respectively. These values are much lower than expected, suggesting that enzymes buried inside the carbon disk would be not operational. Reproportion of the cathode *vs.* anode sizes allowed the increase of the power density to 1.7 mW cm^{-2}. 90% of the EFC performance was maintained after 24 h at 0.8 V, and 54% after 7 days of continuous operation. Performance loss was suggested to be linked to enzyme inactivation, mainly because H_2 depletion during catalysis led to a high local O_2/H_2 ratio.

Up-scaling was made in 2015 by arranging multiple cells in parallel or in series.[149] The OCV and maximum power of a module composed of two stacks of four cells in parallel were 2.09 V and 7.84 mW respectively. The test bed was able to power an electronic clock and five red LEDs during 8 h with no decrease in light intensity. Miniaturization is another challenge for H_2/O_2 EFCs. Wang *et al.* recently reported a miniaturized EFC based on *Ec*Hyd1 and *Mv* BOD immobilized on the carbon electrode and maintained wet within a microvolume of buffer surrounded by an immiscible ionic liquid.[162] Although a low OCV was observed, the small power density recorded, *i.e.* 4 μW cm^{-2}, was stable for 9 h. This configuration allows operation in typically 6 μl of electrolyte, and opens up new avenues towards miniaturization of H_2/O_2 EFCs.

In our group, we first maintained the Nafion membrane separator and worked with 100% H_2 and 100% O_2 in the anodic and cathodic compartments, respectively.[53] Should this membrane be maintained in a future device, the type of separator as a function of the geometry of the cell, and in particular as a function of pH should be particularly examined. *Aa* MbH was used at the anode, allowing it to operate between 25 °C and 80 °C. The concentration of BOD was varied on the cathode in order to study the three operating cell limitations, *i.e.* balance between the anode and cathode, anode limitation or cathode limitation. A potential zone where the EFC could efficiently operate was defined controlled by *Aa* MbH inactivation. The maximum power density was 300 μW cm^{-2} at 0.65 V. The EFC exhibited more than 60% of its power initial value after 24 h of continuous operation at 0.65 V. Otherwise, as amine groups were demonstrated to favour *Aa* MbH orientation, COOHCNTs were replaced by CNTs modified by π–π stacking of an aminopyrene derivative.[57] Membrane-less EFCs were designed with different H_2/air mixtures up to 15% H_2/85% air. Although the CNT film was not optimized, the EFC was demonstrated to operate under such extreme conditions for the hydrogenase,

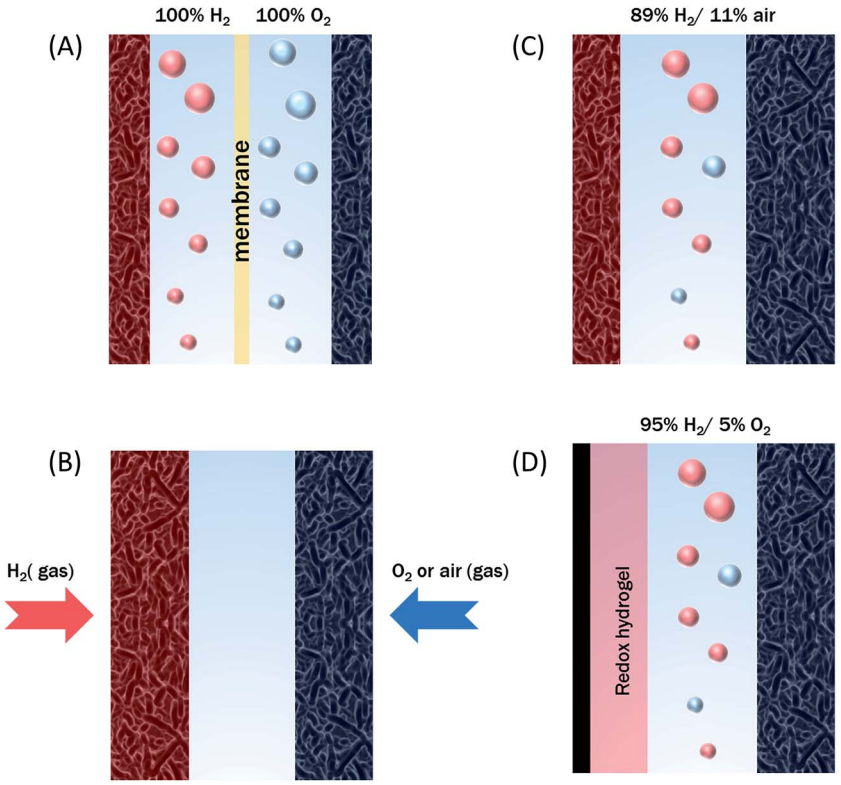

Fig. 12 Main H_2/O_2 EFC configurations. (A) EFC with a membrane separator and direct connection of enzymes; (B) dual gas-diffusion EFC with direct connection of enzymes; (C) membrane-less EFC in low air/H_2 gas mixtures with direct connection of enzymes; (D) membrane-less EFC with direct connection of BOD at the cathode and hydrogenase connected through a redox hydrogel at the anode. In (C) and (D) cathodes are oversized to compensate low cathode substrate availability.

delivering a maximum power of 70 μW cm^{-2}. This is an interesting result, since, as related above, platinum is not very efficient in poor H_2 gas mixtures. Other nanomaterials such as AuNPs were used for the same enzyme immobilization. A maximum power density of 250 μW cm^{-2} at 0.8 V was obtained,[106] but the behavior of *Mv* BOD on AuNPs was shown to severely limit the device. To reach the net power required for a real device, Monsalve *et al.* up scaled the bioelectrodes by using cylinders of carbon felts. Post functionalization by CNTs bearing carboxylic functionalities were suitable for high loading of active *Aa* MbH and *Mv* BOD. The OCV and short circuit current were 1.12 V and 765 μA, respectively. A maximum power of 410 μW was obtained. Associated with suitable electronic circuits, and in particular to a supercapacitor able to store the energy, this EFC was used to power a wireless transmission system. The device powered by the H_2/O_2 EFC was measuring in real time five different parameters and was sending them wirelessly to a laptop every 25 s for 7 h.

The optimal working temperatures of these former EFCs based on *Aa* MbH at the anode were 60 °C and 25 °C in the anodic and cathodic compartments, respectively. The limitation induced by denaturation of *Mv* BOD at temperatures higher than 40 °C was overcome by the use of the thermostable *Bp* BOD at the cathode.[160] In a new EFC, de Poulpiquet *et al.* immobilized the enzymes in carbon nanofibers. A power density of 1.5 mW cm^{-2} was reached at 60 °C. Thanks to the thermostability of both *Aa* MbH and *Bp* BOD, the EFC was proved to be able to operate from 30 to 80 °C, *i.e.* in extreme situation for classical enzymes, enlarging the operational conditions of EFCs.

Are H_2/O_2 EFCs limited to O_2-tolerant hydrogenases on the anodic side? Three different configurations offer the opportunity to enlarge the panel of hydrogenases suitable for the EFC (Fig. 12). The first one takes advantage of the protective role of mesoporous films against O_2 discussed before. Thus, Xu *et al.* designed a membrane-less EFC based on the O_2-sensitive hydrogenase from *E. coli* embedded in compacted CNTs.[149] Under 89% H_2–11% air, the EFC delivered a maximum volumetric power density close to 100 μW cm^{-3} at 0.7 V. The OCV was 1.114 V, a value higher than that one obtained with *Ec*Hyd1, in agreement with the comparative catalytic offsets of both enzymes. However, the stability was much less. More than 50% of the activity was lost after 6 h of operation, compared to 54% remaining activity under the same conditions after 7 days with the *E. coli* O_2-tolerant hydrogenase.

The second configuration consists of air-breathing systems that have been proved to be efficient in fuel cell technology.[164] As this design was shown to be beneficial to prevent hydrogenase from inactivation, hydrogen/air-breathing EFC was evaluated with both O_2-tolerant and O_2-sensitive hydrogenases. Lalaoui *et al.* used *Aa* MbH and *Bp* BOD as thermostable enzymes immobilized on CNTs with suitable surface chemistry as defined above. The membrane-less air-breathing EFC was

operated at 45 °C, and a maximum power density of 0.72 mW cm^{-2} was obtained at 0.6 V. The demonstration of hydrogenase protection by the air-breathing cathode design was even more relevant when an O_2-sensitive hydrogenase was used instead of O_2-tolerant hydrogenases. So *et al.* immobilized the O_2-sensitive *Dv* MF hydrogenase and *Mv* BOD in KB deposited on waterproof carbon cloth.[163] In this case, the anode was also supplied by H_2 as a gas. As discussed before, this configuration was proposed to protect the hydrogenase from anaerobic inactivation. The performances of the bioanode and biocathode were evaluated separately and served to calculate the cell voltage and cell power density. Values of 1.14 V and 8.4 mW cm^{-2} at 0.7 V were calculated, for OCV and power density respectively. The same group further functionalized KB with carboxylic- and amino-functions to fit suitable orientation of *Mv* BOD and *Dv* MH, respectively.[140] Polytetrafluoroethylene was mixed to KB in order to get the required hydrophobicity for gas permeation. Very interestingly, the dual gas-diffusion membrane-less hydrogen/air-breathing EFC displayed a high power density of 6.1 mW cm^{-2} at 0.72 V under quiescent conditions. Nevertheless, anaerobic inactivation of hydrogenase was observed at high current densities due to the hydrogen depletion. While being actively developed and very promising in terms of performance, air-breathing systems are however rarely evaluated for long-term stability of enzymes that might occur in direct contact with gaseous phase in such configuration.

The third configuration is based on the use of low potential redox hydrogels for entrapment of hydrogenases. The above-mentioned EFCs were based on direct connection of enzymes. Here, H_2 oxidation proceeds through a MET process. Plumeré *et al.* constructed a membrane-less H_2/O_2 EFC based on the O_2--sensitive *Dv* MF hydrogenase and *Mv* BOD at the anode and cathode, respectively.[77] To be able to prove the protective role of the redox hydrogels against hydrogenase inactivation under extreme conditions, 95% H_2–5% O_2 gas mixture composition was used, and the cathode was oversized. *Mv* BOD was classically immobilized on carbon modified by carboxylic-functionalized CNTs. Under these conditions, a maximum power density of 180 μW cm^{-2} was obtained, with an OCV of 947 mV. More interestingly, the catalytic current delivered by the bioanode remained unaffected even when the EFC approached short-circuit conditions where the anode potential reaches very high oxidative values. The approach based on viologen-based redox hydrogels was extended to [FeFe] hydrogenase from *Chlamydomonas reinhardtii*, a hydrogenase irreversibly inactivated by O_2. The designed EFC delivered a maximum power density of 225 μW cm^{-2}.[157]

Conclusion and outlook

During the last decade, discovery of new hydrogenases and BODs in the biodiversity, associated with deep understanding of their efficient connection to electrochemical interfaces has allowed us to envision electricity production through H_2/O_2 EFCs (Fig. 12). Although these EFCs were developed later compared to the glucose/O_2 devices, they rapidly outperformed the sugar-based EFCs. This fast improvement is most certainly related to the deep knowledge of the structure of the hydrogenases and the way they behave on electrodes acquired before their use in biotechnological devices. Having a high OCV linked to the nature of oxidant and fuel and the fast kinetics of the enzymes, they nowadays reach power levels compatible with use in real applications. Before commercialization however, there is still a lot of research to be done, to increase short-term and long-term stability and improve electrical connection. These two limitations impose to couple electrochemistry to surface spectroscopy to get a full image of the active enzymes on an electrode surface. Modeling is also required to get a rationalization of the interfaces, to predict a suitable porous matrix for enhanced electrical connection of enzymes and fast substrate diffusion. Recent development in small paper fuel cell would certainly be relevant for EFC designs.[165]

Interestingly, the research in multi-centre redox enzymes has stimulated intensive research in biomimetic inorganic chemistry and artificial enzymes.[166–169] As an example, until recent years, biomimetic catalysts of [NiFe]-hydrogenases were only able to catalyze H_2 oxidation in organic solvents or in acidic aqueous solution.[170,171] Very recently,[172] a nickel–diphosphine complex was immobilized on functionalized CNTs. High activity toward H_2 oxidation over a pH range of 0.3–7 was obtained, with a TOF of 22 s^{-1} at pH 7. A fuel cell was mounted based on this inorganic catalyst at the anode and *Mv* BOD at the cathode. At 25 °C and pH 5, the fuel cell delivered 1.85 mW cm^{-2} at 0.6 V, which compares well with the hydrogenase-based EFCs. Talking about advantages of enzymes over inorganic catalysts, one must be reminded, however, that single enzyme molecule activity outperforms that of platinum or any other chemical catalyst, provided a better long-term stability and more efficient connection are reached. They are widespread in the environment, even more than reported yet, suggesting new properties to be discovered and exploited soon.[19] The occurrence of O_2-tolerant hydrogenases purified from very different microorganisms underlines the relevance of screening biodiversity to look for new enzymes with new properties suitable for H_2/O_2 EFCs, such as tolerance to high potentials, pressure, halides, ionic strength, large range of operational temperatures, low pHs, *etc.* It should also be highly interesting to search for BODs with higher affinity to O_2, higher reduction potentials, or being more active at neutral pHs. Mass production of these enzymes should not be a limitation as soon as commercialization appears on the market. Whatever their future, H_2/O_2 EFC development is a nice example of applicative research which is derived from fundamental ones, and which induces new fundamental research studies in an interdisciplinary approach. Other devices in the energy domain nowadays already take advantage or will take advantage in the close future of the advances in hydrogenase electrochemistry. This is the case of water splitting,[173] CO_2 enzymatic reduction[174] or ammonia-producing H_2/N_2 EFC.[175]

Acknowledgements

The authors thank ANR for financial support (CAROUCELL-ANR-13-BIOME-0003-02). This work was also supported by A*MIDEX Marseille (ANR-11-IDEX-0001-02).

Notes and references

1 M. Rasmussen, S. Abdellaoui and S. Minteer, Enzymatic biofuel cells: 30 years of critical advancements, *Biosens. Bioelectron.*, 2016, **76**, 91–102.

2 A. Yahiro, S. Lee and D. Kimble, Bioelectrochemistry. I. Enzyme utilizing biofuel cell studies, *Biochim. Biophys. Acta*, 1964, **88**, 375–383.

3 A. Babadi, S. Bagheri and S. Hamid, Progress on implantable biofuel cell: nano-carbon functionalization for enzyme immobilization enhancement, *Biosens. Bioelectron.*, 2016, **79**, 850–860.

4 S. Cosnier, A. Gross, A. Le Goff and M. Holzinger, Recent advances on enzymatic glucose/oxygen and hydrogen/oxygen biofuel cells : achievement and limitations, *J. Power Sources*, 2016, **325**, 252–263.

5 N. Mano, J. Fernandez, Y. Kim, W. Shin, A. Bard and A. Heller, Oxygen is electroreduced to water on a « wired » enzyme electrode at a lesser overpotential than on platinum, *J. Am. Chem. Soc.*, 2003, **125**, 15290–15291.

6 S. Cosnier, A. Le Goff and M. Holzinger, Towards glucose biofuel cells implanted in human body for powering artificial organs: review, *Electrochem. Commun.*, 2014, **38**, 19–23.

7 E. Katz and K. MacVittie, Implanted biofuel cells operating *in vivo*-methods, applications and perspectives, *Energy Environ. Sci.*, 2013, **6**, 2791–2803.

8 M. Falk, V. Andoralov, M. Silow, M. Toscano and S. Shleev, Miniature biofuel cell as a potential power source for glucose-sensing contact lenses, *Anal. Chem.*, 2013, **85**, 6342–6348.

9 Y. Ogawa, K. Kato, T. Miyake, K. Nagamine, T. Ofuji, S. Yoshino and M. Nishizawa, Organic transdermal iontophoresis patch with built-in biofuel cell, *Adv. Healthcare Mater.*, 2015, **4**, 506–510.

10 A. de Poulpiquet, D. Ranava, K. Monsalve, M. T. Giudici-Orticoni and E. Lojou, Biohydrogen for a new generation of H_2/O_2 biofuel cells: a sustainable energy perspective, *ChemElectroChem*, 2014, **1**, 1724–1750.

11 P. Chenevier, L. Mugherli, S. Darbe, L. Darchy, S. DiManno, P. Tran, F. Valentino, M. Iannello, A. Volbeda, C. Cavazza and V. Artero, Hydrogenase enzymes: application in biofuel cells and inspiration for the design of noble-metal free catalysts for H_2 oxidation, *C. R. Chim.*, 2013, **16**, 491–505.

12 M. Stephenson and L. Stickland, Hydrogenase: a bacterial enzyme activating molecular hydrogen: the properties of the enzyme, *Biochem. J.*, 1931, **25**, 205–214.

13 S. Tsujimura, M. Fujita, H. Tatsumi, K. Kano and T. Ikeda, Bioelectrocatalysis-based dihydrogen/dioxygen fuel cell operating at physiological pH, *Phys. Chem. Chem. Phys.*, 2001, **3**, 1331–1335.

14 E. Lojou, M. C. Durand, A. Dolla and P. Bianco, Hydrogenase activity control at *Desulfovibrio vulgaris* cell-coated carbon electrodes: biochemical and chemical factors influencing the mediated electrocatalysis, *Electroanalysis*, 2002, **14**, 913–922.

15 B. Pohorelic, J. Voordouw, E. Lojou, A. Dolla, J. Harder and G. Voordouw, Effects of deletion of genes encoding Fe-only hydrogenase of *Desulfovibrio vulgaris* Hildenborough on hydrogen lactate metabolism, *J. Bacteriol.*, 2002, **184**, 679–686.

16 B. Schink and I. Probst, Competitive inhibition of the membrane-bound hydrogenase of *Alcaligenes eutrophus* by molecular oxygen, *Biochem. Biophys. Res. Commun.*, 1980, **95**, 1563–1569.

17 P. Vignais and B. Billoud, Occurrence, classification and biological function of hydrogenases: an overview, *Chem. Rev.*, 2007, **107**, 4206–4272.

18 W. Lubitz, H. Ogata, O. Rüdiger and E. Reijerse, Hydrogenases, *Chem. Rev.*, 2014, **114**, 4081–4148.

19 C. Greening, A. Biswas, C. Carere, C. Jackson, M. Taylor, M. Stott, G. Cook and S. Morales, Genomic and metagenomic surveys of hydrogenase distribution indicate H_2 is a widely utilized energy source for microbial growth and survival, *ISME J.*, 2016, **10**, 761–777.

20 H. Shafaat, O. Rüdiger, H. Ogata and W. Lubitz, [NiFe] hydrogenases: a common active site for hydrogen metabolism under diverse conditions, *Biochim. Biophys. Acta*, 2013, **1827**, 986–1002.

21 H. Ogata, W. Lubitz and Y. Higuchi, Structure and function of [NiFe] hydrogenases, *J. Biochem.*, 2016, **160**, 251–258.

22 L. Flanagan and A. Parkin, Electrochemical insights into the mechanism of NiFe membrane-bound hydrogenases, *Biochem. Soc. Trans.*, 2016, **44**, 315–328.

23 R. Evans, E. Brooke, S. Wehlin, E. Nomerotskaia, F. Sargent, S. Carr, S. Phillips and F. Armstrong, Mechanism of hydrogen activation by [NiFe] hydrogenases, *Nat. Chem. Biol.*, 2016, **12**, 46–50.

24 C. Greco, V. Fourmond, C. Baffert, P. Wang, S. Dementin, P. Bertrand, M. Bruschi, J. Blumberger, L. de Gioia and C. Leger, Combining experimental and theoretical methods to learn about the reactivity of gas-processing metalloenzymes, *Energy Environ. Sci.*, 2014, **7**, 3543–3573.

25 E. Solomon, U. Sundaram and T. Machonkin, Multicopperoxidases and oxygenases, *Chem. Rev.*, 1996, **96**, 2563–2605.

26 E. Solomon, A. Augustine and J. Yoon, O_2 reduction to H_2O by the multicopper oxidases, *Dalton Trans.*, 2008, 3921–3932.

27 E. Solomon, Dioxygen binding, activation, and reduction to H_2O by Cu enzymes, *Inorg. Chem.*, 2016, **55**, 6364–6375.

28 H. Komori and Y. Higuchi, Structural insights into the O_2 reduction mechanism of multicopper oxidase, *J. Biochem.*, 2015, **158**, 293–298.

29 N. Mano and L. Edembe, Bilirubin oxidases in bioelectrochemistry: features and recent findings, *Biosens. Bioelectron.*, 2013, **50**, 478–485.

30 F. Tasca, D. Farias, C. Castro, C. Acuna-Rougier and R. Antiochia, Bilirubin oxidase from Myrothecium verrucaria physically absorbed on graphite electrodes. Insights into the alternative resting form and the sources of activity loss, *PLoS One*, 2015, **10**, e0132181.

31 M. Dagys, A. Laurynenas, D. Ratautas, J. Kulys, R. Vidziunaite, M. Talaikis, G. Niaura, L. Marcinkeviciene, R. Meskys and S. Shleev, Oxygen electroreduction catalysed by lacase wired to gold nanoparticle *via* trinuclear copper cluster, *Energy Environ. Sci.*, 2017, **10**, 498–502.

32 A. de Poulpiquet, C. Kjaergaard, J. Rouhana, I. Mazurenko, P. Infossi, S. Gounel, R. Gadiou, M. T. Giudici-Orticoni, E. Solomon, N. Mano and E. Lojou, Mechanism of chloride inhibition of bilirubin oxidases and its dependence on potential and pH, *ACS Catal.*, 2017, **7**, 3916–3926.

33 P. Agbo, J. Heath and H. Gray, Modeling dioxygen reduction at multicopper oxidase cathodes, *J. Am. Chem. Soc.*, 2014, **136**, 13882–13887.

34 S. Varfolomeev, A. Yaropolov, I. Berezin, M. Tarasevich and V. Bogdanovskaya, Bioelectrocatalysis. Hydrogenase as catalyst of electrochemical hydrogen ionization, *Bioelectrochem. Bioenerg.*, 1977, **4**, 314–326.

35 F. Armstrong, H. Hill and N. Walton, Direct electrochemistry of redox proteins, *Acc. Chem. Res.*, 1988, **21**, 407–413.

36 A. Heller, Electron-conducting redox hydrogels: design, characteristics and synthesis, *Curr. Opin. Chem. Biol.*, 2006, **10**, 664–672.

37 J. Masa and W. Schuhmann, Electrocatalysis and bioelectrocatalysis – Distinction without a difference, *Nano Energy*, 2016, **29**, 466–475.

38 K. Vincent, A. Parkin and F. Armstrong, Investigating and exploiting the electrocatalytic properties of hydrogenases, *Chem. Rev.*, 2007, **107**, 4366–4413.

39 J. Cracknell, K. Vincent and F. Armstrong, Enzymes as working or inspirational electrocatalysts for fuel cells and electrolysis, *Chem. Rev.*, 2008, **108**, 2439–2461.

40 L. Dos Santos, V. Climent, C. Blanford and F. Armstrong, Mechanistic studies of the blue Cu enzyme, bilirubin oxidase, as a highly efficient electrocatalyst for the oxygen reduction reaction, *Phys. Chem. Chem. Phys.*, 2010, **12**, 13962–13974.

41 M. Tominaga, A. Sasaki and M. Togami, Laccase bioelectrocatalyst at a steroid-type biosurfactant-modified carbon nanotube surface, *Anal. Chem.*, 2015, **87**, 5417–5421.

42 S. Shleev, V. Andoralov, D. Pankratov, M. Falk, O. Aleksejeva and Z. Blum, Oxygen electroreduction *versus* bioelectroreduction: direct electron transfer approach, *Electroanalysis*, 2016, **28**, 2270–2287.

43 A. Christenson, S. Shleev, N. Mano, A. Heller and L. Gorton, Redox potentials of the blue active sites of bilirubin oxidases, *Biochim. Biophys. Acta, Bioenerg.*, 2006, **1757**, 1634–1641.

44 N. Mano, V. Soukharev and A. Heller, A laccase-wiring redox hydrogel for efficient catalysis of O_2 electroreduction, *J. Phys. Chem. B*, 2006, **110**, 11180–11187.

45 A. Jones, E. Sillery, S. Albracht and F. Armstrong, Direct comparison of the electrocatalytic oxidation of hydrogen by an enzyme and a platinum electrode, *Chem. Commun.*, 2002, 866–867.

46 A. Karyakin, S. Morozov, O. Voronin, N. Zorin, E. Karyakina, V. Fateyev and S. Cosnier, The limiting performance characteristics in bioelectrocatalysis of hydrogenase enzymes, *Angew. Chem., Int. Ed.*, 2007, **46**, 7244–7246.

47 T. Woolerton and K. Vincent, Oxidation of dilute H_2 and H_2/O_2 mixtures by hydrogenases and Pt, *Electrochim. Acta*, 2009, **54**, 5011–5017.

48 K. Vincent, J. Cracknell, O. Lenz, I. Zebger, B. Friedrich and F. Armstrong, Electrocatalytic hydrogen oxidation by an enzyme at high carbon monoxide or oxygen levels, *Proc. Natl. Acad. Sci. U. S. A.*, 2005, **102**, 16951–16954.

49 K. Vincent, J. Cracknell, J. Clark, M. Ludwig, O. Lenz, B. Friedrich and F. Armstrong, Electricity from low-level H_2 in still air – an ultimate test for an oxygen tolerant hydrogenase, *Chem. Commun.*, 2006, 5033–5035.

50 M. Lukey, A. Parkin, M. Roessler, B. Murphy, J. Harmer, T. Palmer, F. Sargent and F. Armstrong, How *Escherichia coli* is equipped to oxidize hydrogen under different redox conditions, *J. Biol. Chem.*, 2010, **285**, 3928–3938.

51 A. Wait, A. Parkin, G. Morley, L. dos Santos and F. Armstrong, Characteristics of enzyme-based hydrogen fuel cells using an oxygen-tolerant hydrogenase as the anodic catalyst, *J. Phys. Chem.*, 2010, **114**, 12003–12009.

52 M. Pandelia, V. Fourmond, P. Tron-Infossi, E. Lojou, P. Bertrand, C. Leger, M. T. Giudici-Orticoni and W. Lubitz, Membrane-bound hydrogenase I from the hyperthermophilic bacterium *Aquifex aeolicus*: enzyme activation, redox intermediates and oxygen tolerance, *J. Am. Chem. Soc.*, 2010, **132**, 6991–7004.

53 A. Ciaccafava, A. de Poulpiquet, V. Techer, M. T. Giudici-Orticoni, S. Tingry, C. Innocent and E. Lojou, An innovative powerful and mediatorless H_2/O_2 biofuel cell based on an outstanding bioanode, *Electrochem. Commun.*, 2012, **23**, 25–28.

54 A. Parkin, L. Bowman, M. Roessler, R. Davies, T. Palmer, F. Armstrong and F. Sargent, How *Salmonella* oxidises H_2 under aerobic conditions, *FEBS Lett.*, 2012, **586**, 536–544.

55 M. Brugna-Guiral, P. Tron, W. Nitschke, K.-O. Stetter, B. Burlat, B. Guigliarelli, M. Bruschi and M. T. Giudici-Orticoni, [NiFe] hydrogenases from the hyperthermophilic bacterium *Aquifex aeolicus*: properties, function, and phylogenetics, *Extremophiles*, 2003, **7**, 145–157.

56 X. Luo, P. Tron-Infossi, M. Brugna, M. T. Giudici-Orticoni and E. Lojou, Immobilization of the hyperthermophilic hydrogenase from *Aquifex aeolicus* bacterium onto gold and carbon nanotube electrodes for efficient H_2 oxidation, *J. Biol. Inorg Chem.*, 2009, **14**, 1275–1288.

57 K. Monsalve, I. Mazurenko, C. Gutierrez-Sanchez, M. Ilbert, P. Infossi, S. Frielingsdorf, M. T. Giudici-Orticoni, O. Lenz and E. Lojou, Impact of Carbon Nanotube Surface Chemistry on Hydrogen Oxidation by membrane-bound oxygen-tolerant hydrogenases, *ChemElectroChem.*, 2016, **3**, 2179–2188.

58 K.-S. Yoon, K. Fukuda, K. Fujisawa and H. Nishihara, Purification and characterization of a highly thermostable, oxygen-resistant, respiratory [NiFe]-hydrogenase from a marine, aerobic, hydrogen-oxidizing

bacterium Hydrogenovibrio marinus, *Int. J. Hydrogen Energy*, 2011, **36**, 7081–7088.

59 J. Fritsch, P. Scheerer, S. Frielingsdorf, S. Kroschinsky, B. Friedrich, O. Lenz and C. Spahn, The crystal structure of an oxygen-tolerant hydrogenase uncovers a novel iron-sulphur centre, *Nature*, 2011, **479**, 249–252.

60 Y. Shomura, K. Yoon, H. Nishihara and Y. Higuchi, Structural basis for a [4Fe-3S] cluster in the oxygen-tolerant membrane-bound [NiFe]-hydrogenase, *Nature*, 2011, **479**, 253–256.

61 A. Volbeda, P. Amara, C. Darnault, J. Mouesca, A. Parkin, M. Roessler, F. Armstrong and J. Fontecilla-Camps, X-ray crystallographic and computational studies of the O_2-tolerant [NiFe]-hydrogenase 1 from *Escherichia coli*, *Proc. Natl. Acad. Sci. U. S. A.*, 2012, **109**, 5305–5310.

62 L. Bowman, L. Flanagan, P. Fyfe, A. Parkin, W. Hunter and F. Sargent, How the structure of the large subunit controls function in an oxygen-tolerant [NiFe]-hydrogenase, *Biochem. J.*, 2014, **458**, 449–458.

63 J. Fritsch, O. Lenz and B. Friedrich, Structure, function and biosynthesis of O_2-tolerant hydrogenases, *Nat. Rev. Microbiol.*, 2013, **11**, 106–114.

64 F. Armstrong, R. Evans, S. Hexter, B. Murphy, M. Roessler and P. Wulff, Guiding principles of hydrogenase catalysis instigated and clarified by protein film electrochemistry, *Acc. Chem. Res.*, 2016, **49**, 884–892.

65 E. Brooke, R. Evans, S. Islam, G. Roberts, S. Wehlin, S. Carr, S. Phillips and F. Armstrong, Importance of the active site "canopy" residues in an O_2-tolerant [NiFe]-hydrogenase, *Biochemistry*, 2017, **56**, 132–142.

66 A. Hamdan, P. P. Liebgott, V. Fourmond, O. Gutierrez-Sanz, A. De Lacey, P. Infossi, M. Rousset, S. Dementin and C. Léger, Relation between anaerobic inactivation and oxygen tolerance in a large series of NiFe hydrogenase mutants, *Proc. Natl. Acad. Sci. U. S. A.*, 2012, **109**, 19916–19921.

67 P. Wulff, C. Thomas, F. Sargent and F. Armstrong, How the oxygen tolerance of a [NiFe]-hydrogenase depends on quaternary structure, *J. Biol. Inorg Chem.*, 2016, **21**, 121–134.

68 E. Suraniti, S. Tsujimura, F. Durand and N. Mano, Thermophilic biocathode with bilirubin oxidase from *Bacillus pumilus*, *Electrochem. Commun.*, 2013, **26**, 41–44.

69 F. Durand, S. Gounel, C. Kjaergaard, E. Solomon and N. Mano, Bilirubin oxidase from *Magnaporthe oryzae*: an attractive new enzyme for biotechnological applications, *Appl. Microbiol. Biotechnol.*, 2012, **96**, 1489–1498.

70 I. Mazurenko, K. Monsalve, J. Rouhana, P. Parent, C. Laffon, A. Le Goff, S. Szunerits, R. Boukherroub, M. T. Giudici-Orticoni, N. Mano and E. Lojou, How the Intricate Interactions between Carbon Nanotubes and Two Bilirubin Oxidases Control Direct and Mediated O_2 Reduction, *ACS Appl. Mater. Interfaces*, 2016, **8**, 23074–23085.

71 A. Volbeda, C. Damault, A. Parkin, F. Sargent, F. Armstrong and J. Fontecilla-Camps, Crystal structure of the O_2-tolerant membrane-bound hydrogenase 1 from *Escherichia coli* in complex with its cognate cytochrome *b*, *Structure*, 2013, **21**, 184–190.

72 A. Ciaccafava, C. Hamon, P. Infossi, V. Marchi, M. T. Giudici-Orticoni and E. Lojou, Light-induced reactivation of O_2-tolerant membrane-bound [Ni-Fe] hydrogenase from the hyperthermophilic bacterium *Aquifex aeolicus* under turnover conditions, *Phys. Chem. Chem. Phys.*, 2013, **39**, 16463–16467.

73 C. Hamon, A. Ciaccafava, P. Infossi, R. Puppo, P. Even-Hernandez, E. Lojou and V. Marchi, Synthesis and Enzymatic activity of an O_2 resistant hydrogenase/CdSe@CdS quantum rod bioconjugate, *Chem. Commun.*, 2014, **50**, 4989–4992.

74 K. So, Y. Kitazumi, O. Shirai, K. Kurita, H. Nishihara, Y. Higuchi and K. Kano, Gas-diffusion and direct-electron-transfer-type bioanode for hydrogen oxidation with oxygen-tolerant [NiFe]-hydrogenase as an electrocatalyst, *Chem. Lett.*, 2014, **43**, 1575–1577.

75 K. So, Y. Kitazumi, O. Shirai, K. Kurita, H. Nishihara, Y. Higuchi and K. Kano, Kinetic analysis of inactivation and enzyme reaction of oxygen-tolerant [NiFe]-hydrogenase at direct electron-transfer anode, *Bull. Chem. Soc. Jpn.*, 2014, **87**, 1177–1185.

76 V. Radu, S. Frielingsdorf, S. Evans, O. Lenz and L. Jeuken, Enhances oxygen-tolerance of the full heterotrimeric membrane-bound [NiFe]-hydrogenase of Ralstonia eutropha, *J. Am. Chem. Soc.*, 2014, **136**, 8512–8515.

77 N. Plumeré, O. Rüdiger, A. Oughli, R. Williams, J. Vivekananthan, S. Pöller, W. Lubitz and W. Schuhmann, A redox hydrogel protects hydrogenase from high-potential deactivation and oxygen damage, *Nat. Chem.*, 2014, **6**, 822–827.

78 J. Baur, A. Le Goff, S. Dementin, M. Holzinger, M. Rousset and S. Cosnier, Three-dimensional carbon nanotube-polypyrrole-[NiFe] hydrogenase electrodes for the efficient electrocatalytic oxidation of H_2, *Int. J. Hydrogen Energy*, 2011, **36**, 12096–12101.

79 A. Walcarius, S. Minteer, J. Wang, Y. Lin and A. Merkoci, Nanomaterials for bio-functionalized electrodes: recent trends, *J. Mater. Chem. B*, 2013, **1**, 4878–4908.

80 A. de Poulpiquet, A. Ciaccafava and E. Lojou, New trends in enzyme immobilization at nanostructured interfaces for efficient electrocatalysis in biofuel cells, *Electrochim. Acta*, 2014, **126**, 104–114.

81 S. Minteer, P. Atanassov, H. Luckarift and G. Johnson, New materials for biological fuel cells, *Mater. Today*, 2012, **15**, 166–173.

82 R. Milton, T. Wang, K. Knoche and S. Minteer, Tailoring biointerfaces for electrocatalysis, *Langmuir*, 2016, **32**, 2291–2301.

83 J. Quinson, R. Hidalgo, P. Ash, F. Dillon, N. Grobert and K. Vincent, Comparison of carbon materials as electrodes for enzyme electrocatalysis: hydrogenase as a case study, *Faraday Discuss.*, 2014, **172**, 473–496.

84 P. Unwin, A. Güell and G. Zhang, Nanoscale electrochemistry of sp^2 carbon materials: from graphite

and graphene to carbon nanotubes, *Acc. Chem. Res.*, 2016, **49**, 2041–2048.
85 A. Geim and K. Novoselov, The rise of graphene, *Nat. Mater.*, 2007, **6**, 183–191.
86 J. Filip and J. Tkac, Is graphene worth using in biofuel cells?, *Electrochim. Acta*, 2014, **136**, 340–354.
87 A. Navaee, A. Salimi and F. Jafari, Electrochemical pretreatment of amino-carbon nanotubes on graphene support as a novel platform for bilirubin oxidase with improved bioelectrocataytic activity towards oxygen reduction, *Chem.–Eur. J.*, 2015, **21**, 4949–4953.
88 A. Campbell, M. Jose, S. Marx, S. Cornelius, R. Koepsel, M. Islam and A. Russel, Improved power density of an enzymatic biofuel cell with fibrous supports of high curvatures, *RSC Adv.*, 2016, **6**, 10150–10158.
89 C. Di Bari, A. Goni-Urtiaga, M. Pita, S. Shleev, M. Toscano, R. Sainz and A. De Lacey, Fabrication of high surface area graphene electrodes with high performance towards enzymatic oxygen reduction, *Electrochim. Acta*, 2016, **191**, 500–509.
90 J. Filip, A. Andicsova-Eckstein, A. Vikartovska and J. Tkac, Immobilization of bilirubin oxidase on graphene oxide flakes with different negative charge density for oxygen reduction. The effect of GO charge density on enzyme coverage, electron transfer rate and current density, *Biosens. Bioelectron.*, 2017, **89**, 384–389.
91 N. Lalaoui, A. Le Goff, M. Holzinger and S. Cosnier, Fully oriented bilirubin oxidase on porphyrin-functionalized carbon nanotube electrodes for electrocatalytic oxygen reduction, *Chem.–Eur. J.*, 2015, **21**, 16868–16873.
92 M. A. Alonso-Lomillo, O. Rudiger, A. Maroto-Valiente, M. Velez, I. Rodriguez-Ramos, F. Munoz, V. Fernandez and A. De Lacey, Hydrogenase-coated carbon nanotubes for efficient H_2 oxidation, *Nano Lett.*, 2007, **7**, 1603–1608.
93 F. Hoeben, I. Heller, S. Albracht, C. Dekker, S. Lemay and H. Heering, Polymyxin-coated an and carbon nanotube electrodes for stable [NiFe]-hydrogenase film voltammetry, *Langmuir*, 2008, **24**, 5925–5931.
94 E. Lojou, X. Luo, N. Candoni, M. Brugna, S. Dementin and M. T. Giudici-Orticoni, Hydrogenases as biocatalysts for biofuel cells: efficient H_2 oxidation at electrodes modified with carbon nanotubes, *J. Biol. Inorg Chem.*, 2008, **13**, 1157–1167.
95 S. Krishnan and F. Armstrong, Order-of-magnitude enhancement of an enzymatic hydrogen-air fuel cell based on pyrenyl carbon nanostructures, *Chem. Sci.*, 2012, **3**, 1015–1023.
96 A. de Poulpiquet, A. Ciaccafava, K. Szot, B. Pillain, P. Infossi, M. Guiral, M. Opallo, M. T. Giudici-Orticoni and E. Lojou, Exploring properties of a hyperthermophilic membrane-bound hydrogenase at carbon nanotube modified electrodes for a powerful H_2/O_2 biofuel cell, *Electroanalysis*, 2013, **25**, 685–695.
97 A. de Poulpiquet, A. Ciaccafava, S. Benomar, M. T. Giudici-Orticoni and E. Lojou, in *Synthesis and applications of carbon nanotubes and their composites*, ed. S. Suzuki, Intech, 2013, pp. 433–466.
98 W. Zhang, S. Zhu, R. Luque, S. Han, L. Hu and G. Xu, Recent development of carbon electrode materials and their bioanalytical and environmental applications, *Chem. Soc. Rev.*, 2016, **45**, 715–752.
99 K. Zelechowska, B. Trawinski, S. Draminska, D. Majdecka, R. Bilewicz and B. Kusz, Oxygen biosensor based on carbon nanotubes directly grown on graphitic substrate, *Sens. Actuators, B*, 2017, **240**, 1308–1313.
100 B. Reuillard, A. Le Goff, C. Agnes, M. Holzinger, A. Zebda, C. Gondran, K. Elouarzaki and S. Cosnier, High power enzymatic biofuel cell based on naphthoquinone-mediated oxidation of glucose by glucose oxidase in a carbon nanotube 3D matrix, *Phys. Chem. Chem. Phys.*, 2013, **15**, 4892–4896.
101 S. Babanova, K. Artyushkova, Y. Ulyanova, S. Singhal and P. Atanassov, Design of experiments and principal component analysis as approaches for enhancing performance of gas-diffusional air-breathing bilirubin oxidase cathode, *J. Power Sources*, 2014, **245**, 389–397.
102 F. Giroud, R. Milton, B. Tan and S. Minteer, Simplifying Enzymatic Biofuel Cells: Immobilized Naphthoquinone as a Biocathodic Orientational Moiety and Bioanodic Electron Mediator, *ACS Catal.*, 2015, **5**, 1240–1244.
103 A. de Poulpiquet, H. Marques-Knopf, V. Wernert, R. Gadiou, M. T. Giudici-Orticoni and E. Lojou, Carbon Nanofiber Mesoporous Films: Efficient Platforms for Bio-Hydrogen Oxidation in Biofuel Cells, *Phys. Chem. Chem. Phys.*, 2014, **16**, 1366–1378.
104 S. Tsujimura, E. Suraniti, F. Durand and N. Mano, Oxygen reduction reactions of the thermostable bilirubin oxidase from *Bacillus pumilus* on mesoporous carbon-cryogel electrodes, *Electrochim. Acta*, 2014, **117**, 263–267.
105 S. Fujita, S. Yamanoi, K. Murata, H. Mita, T. Samukawa, T. Nakagawa, H. Sakai and Y. Tokita, A repeatedly refuelable mediated biofuel cell based on a hierarchical porous carbon electrode, *Sci. Rep.*, 2014, **4**, 4937.
106 K. Monsalve, M. Roger, C. Gutierrez-Sanchez, M. Ilbert, S. Nitsche, D. Byrne-Kodjabachian, V. Marchi and E. Lojou, Hydrogen bioelectrooxidation on gold nanoparticle-based electrodes modified by *Aquifex aeolicus* hydrogenase: application to hydrogen/oxygen enzymatic biofuel cells, *Bioelectrochemistry*, 2015, **106**, 47–55.
107 V. Flexer, N. Brun, M. Destribats, R. Backov and N. Mano, A novel three-dimensional macrocellular carbonaceous biofuel cell, *Phys. Chem. Chem. Phys.*, 2013, **15**, 6437–6445.
108 J. Vivekananthan, R. Rincon, V. Kuznetsov, S. Pöller and W. Schuhmann, Biofuel-cell cathodes based on bilirubin oxidase immobilized through organic linkers on 3D hierarchically structured carbon electrodes, *ChemElectroChem.*, 2014, **1**, 1901–1908.
109 K. Monsalve, I. Mazurenko, N. Lalaoui, A. Le Goff, M. Holzinger, P. Infossi, S. Nitsche, J. Y. Lojou, M. T. Giudici-Orticoni, S. Cosnier and E. Lojou, A H_2/O_2 enzymatic fuel cell as a sustainable power for a wireless device, *Electrochem. Commun.*, 2015, **60**, 216–220.

110 C. Mateo-Mateo, A.-S. Michardière, S. Gounel, I. Ly, J. Rouhana, P. Poulin and N. Mano, Wet-spun bioelectronic fibers of imbricated enzymes and carbon nanotubes for efficient microelectrodes, *ChemElectroChem.*, 2015, **2**, 1908–1912.

111 A. Engel, C. Both, A. Cherifi, S. Tingry, D. Cornu, A. Peigney and C. Laurent, Enhanced performance of electrospun carbon fibers modified with carbon nanotubes: promising electrodes for enzymatic biofuel cells, *Nanotechnology*, 2013, **24**, 245402.

112 S. Tsujimura and K. Murata, Electrochemical oxygen reduction catalyzed by bilirubin oxidase with the aid of 2,2′-azinobis(3-ethylbenzothiazolin-6-sulfonate) on a MgO-template carbon electrode, *Electrochim. Acta*, 2015, **180**, 555–559.

113 J. Polte, Fundamental growth principles of colloidal metal nanoparticles – a new perspective, *CrystEngComm*, 2015, **17**, 6809–6830.

114 D. Pankratov, R. Sundberg, D. Suyatin, J. Sotres, A. Barrantes, T. Ruzgas, I. Maximov, L. Montelius and S. Shleev, The influence of nanoparticles on enzymatic bioelectrocatalysis, *RSC Adv.*, 2014, **4**, 38164–38168.

115 U. Salaj-Kosla, S. Pöller, Y. Beyl, M. D. Scanlon, S. Beloshapkin, S. Shleev, W. Schuhmann and E. Magner, Direct electron transfer of bilirubin oxidase at an unmodified nanoporous gold biocathode, *Electrochem. Commun.*, 2012, **16**, 92–95.

116 T. Siepenkoetter, U. Salaj-Kosla, X. Xiao, S. Belochapkine and E. Magner, Nanoporous gols electrodes with tuneable pore sizes for bioelectrochemical applications, *Electroanalysis*, 2016, **28**, 2415–2423.

117 G. Martin, S. Minteer and M. Cooney, Spatial distribution of malate dehydrogenase in chitosan scaffolds, *ACS Appl. Mater. Interfaces*, 2009, **1**, 367–372.

118 L. Xu and F. Armstrong, Optimizing the power of enzyme-based membrane-less hydrogen fuel cells for hydrogen-rich H_2–air mixtures, *Energy Environ. Sci.*, 2013, **6**, 2166–2171.

119 C. Leger, A. Jones, S. Albracht and F. Armstrong, *J. Phys. Chem. B*, 2002, **106**, 13058–13063.

120 S. Hexter, F. Gray, T. Happe, V. Climent and F. Armstrong, *Proc. Natl. Acad. Sci. U. S. A.*, 2012, **109**, 11516–11521.

121 M. Roger, A. de Poulpiquet, A. Ciaccafava, M. Ilbert, M. Guiral, M. T. Giudici-Orticoni and E. Lojou, Reconstitution of supramolecular organization involved in energy metabolisms at electrochemical interfaces for biosensing and bioenergy production, *Anal. Bioanal. Chem.*, 2014, **406**, 1011–1027.

122 A. Ciaccafava, P. Infossi, M. Ilbert, M. Guiral, S. Lecomte, M. T. Giudici-Orticoni and E. Lojou, Electrochemistry, AFM and PM-IRRAS spectroscopy of immobilized hydrogenase: role of a trans-membrane helix on enzyme orientation for efficient H_2 oxidation, *Angew. Chem., Int. Ed.*, 2012, **51**, 953–956.

123 A. Ciaccafava, A. De Poulpiquet, P. Infossi, S. Robert, R. Gadiou, M. T. Giudici-Orticoni, S. Lecomte and E. Lojou, A friendly detergent for H_2 oxidation by Aquifex aeolicus membrane-bound hydrogenase immobilized on graphite and SAM-modified gold electrodes, *Electrochim. Acta*, 2012, **82**, 115–125.

124 F. Oteri, M. Baaden, E. Lojou and S. Sacquin-Mora, Multiscale simulations give insight into the hydrogen in- and out-pathways of [NiFe] hydrogenases from *Aquifex aeolicus* and *Desulfovibrio fructosovorans*, *J. Phys. Chem. B*, 2014, **118**, 13800–13811.

125 N. Heidary, T. Utesch, M. Zerball, M. Horch, D. Millo, J. Fritsch, O. Lenz, R. von Klitzing, P. Hildebrandt, A. Fischer, M. A. Mroginski and I. Zebger, Orientation-Controlled Electrocatalytic Efficiency of an Adsorbed Oxygen-Tolerant Hydrogenase, *PLoS One*, 2015, **10**, e0143101.

126 J. Cracknell, J. A. T. McNamara, E. Lowe and C. Blanford, Bilirubin oxidase from *Myrothecium verrucaria*: X-ray determination of the complete crystal structure and a rational surface modification for enhanced electrocatalytic O_2 reduction, *Dalton Trans.*, 2011, **40**, 6668–6675.

127 C. Gutierrez-Sanchez, A. Ciaccafava, P. Y. Blanchard, K. Monsalve, M. T. Giudici-Orticoni, S. Lecomte and E. Lojou, Efficiency of Enzymatic O_2 Reduction by Myrothecium verrucaria Bilirubin Oxidase Probed by Surface Plasmon Resonance, PMIRRAS, and Electrochemistry, *ACS Catal.*, 2016, **6**, 5482–5492.

128 P. Ramirez, N. Mano, R. Andreu, T. Ruzgas, A. Heller, L. Gorton and S. Shleev, Direct electron transfer from graphite and functionalized gold electrodes to T1 and T2/T3 copper centers of bilirubin oxidase, *Biochim. Biophys. Acta*, 2008, **1777**, 1364–1369.

129 Y. Sugimoto, Y. Kitazumi, O. Shirai and K. Kano, Effects of mesoporous structures on direct electron transfer-type bioelectrocatalysis: facts and simulation on a three-dimensional model of random orientation of enzymes, *Electrochemistry*, 2017, **85**, 82–87.

130 Y. Matanovic, S. Babanova, M. Seow Chavez and P. Atanassov, Protein-support interactions for rationally designed bilirubin oxidase based cathode: a computational study, *J. Phys. Chem. B*, 2016, **120**, 3634–3641.

131 R. Lopez, S. Babanova, Y. Ulyanova, S. Singhal and P. Atanassov, Improved interfacial electron transfer in modified bilirubin oxidase biocathodes, *ChemElectroChem*, 2014, **1**, 241–248.

132 Y. Ulyanova, S. Babanova, E. Pinchon, I. Matanovic, S. Singhal and P. Atanassov, Effect of enzymatic orientation through the use of syringaldazine molecules on multiple multi-copper oxidase enzymes, *Phys. Chem. Chem. Phys.*, 2014, **16**, 13367–13375.

133 N. Lalaoui, M. Holzinger, A. Le Goff and S. Cosnier, Diazonium functionalisation of carbon nanotubes for specific orientation of multicopper oxidases : controlling electron entry points and oxygen diffusion to the enzyme, *Chem.–Eur. J.*, 2016, **22**, 10494–10500.

134 F. Giroud, K. Sawada, M. Taya and S. Cosnier, 5,5′-Dthiobis(2-nitrobenzoic acid) pyrene derivative-carbon

nanotube electrodes for NADH electrooxidation and oriented immobilization of multicopper oxidases for the development of glucose/O_2 biofuel cells, *Biosens. Bioelectron.*, 2017, **87**, 957–963.

135 C. Kjaergaard, S. Jones, S. Gounel, N. Mano and E. Solomon, Two-electron reduction *versus* one-electron oxidation of the type 3 pair in the multicopper oxidases, *J. Am. Chem. Soc.*, 2015, **137**, 8783–8794.

136 T. Le, V. Flaud, M. Bechelany, M. Cretin and S. Tingry, Optimal direct electron transfer between MWCNTs@COOH/BOD/chitosan layer and porous carbon felt for dioxygen reduction, *Electrochim. Acta*, 2017, **230**, 373–381.

137 K. So, M. Onizuka, T. Komukai, Y. Kitazumi, O. Shirai and K. Kano, Significance of the length of carbon nanotubes on the bioelectrocatalytic activity of bilirubin oxidase for dioxygen reduction, *Electrochim. Acta*, 2016, **192**, 133–138.

138 K. So, S. Kawai, Y. Hamano, Y. Kitazumi, O. Shirai, M. Hibi, J. Ogawa and K. Kano, Improvement of a direct electron transfer-type fructose/dioxygen biofuel cell with a substrate-modified electrode, *Phys. Chem. Chem. Phys.*, 2014, **16**, 4823–4829.

139 K. So, Y. Kitazumi, O. Shirai and K. Kano, Analysis of factors governing direct electron transfer-type bioelectrocatalysis of bilirubin oxidase at modified electrodes, *J. Electroanal. Chem.*, 2016, **783**, 316–323.

140 H.-Q. Xia, K. So, Y. Kitazumi, O. Shirai, K. Nishikawa, Y. Higuchi and K. Kano, Dual gas-diffusion membrane- and mediatorless dihydrogen/air-breathing biofuel cell operating at room temperature, *J. Power Sources*, 2016, **335**, 105–112.

141 F. Oteri, A. Ciaccafava, A. de Poulpiquet, E. Lojou, M. Baaden and S. Sacquin-Mora, Fluctuations in the dipole moment of membrane-bound hydrogenase from *Aquifex aeolicus* account for its adaptability to charged electrodes, *Phys. Chem. Chem. Phys.*, 2014, **16**, 11318–11322.

142 K. Sokol, D. Mersch, V. Hartmann, J. Zhang, M. Nowaczyk, M. Rogner, A. Ruff, W. Schuhmann, N. Plumere and E. Reisner, Rational wiring of photosystem II to hierarchical indium tin oxide electrodes using redox polymers, *Energy Environ. Sci.*, 2016, **9**, 3698–3709.

143 J. Liu, W.-J. Wu, F. Fang, N. Zorin, M. Chen and D.-J. Qian, Immobilization of hydrogenase on carbon nanotube polyelectrolytes as heterogeneous catalysts for electrocatalytic interconversion of protons and hydrogen, *J. Nanopart. Res.*, 2016, **18**, 220.

144 H. Shin and C. Kang, Enhanced performance of the wired-bilirubin oxidase oxygen cathode with incorporation of carboxylated single-walled carbon nanotubes, *Electrochim. Acta*, 2014, **115**, 599–606.

145 T. Siepenkoetter, U. Salaj-Kosla, X. Xiao, P. O Conghaile, M. Pita, R. Ludwig and E. Magner, Immobilization of redox enzymes on nanoporous gold electrodes: applications in biofuel cells, *ChemPlusChem*, 2017, **82**, 553–560.

146 P. Saboe, P. Owen, E. Conte, M. Farell, G. C. Bazan and M. Kumar, Biomimetic and Bioinspired Approaches for Wiring Enzymes to Electrode Interfaces, *Energy Environ. Sci.*, 2017, **10**, 14–42.

147 K. Singh, T. McArdle, P. Sullivan and C. Blanford, Sources of activity loss in the fuel cell enzyme bilirubin oxidase, *Energy Environ. Sci.*, 2013, **6**, 2460–2464.

148 T. McArdle, T. McNamara, F. Fei, K. Singh and C. Blanford, Optimizing the mass-specific activity of bilirubin oxidase adlayers through combined electrochemical quartz crystal microbalance and dual polarization interferometry analyses, *ACS Appl. Mater. Interfaces*, 2015, **7**, 25270–25280.

149 L. Xu and F. Armstrong, Pushing the limits for enzyme-based membrane-less hydrogen fuel cells - achieving useful power and stability, *RSC Adv.*, 2015, **5**, 3649–3656.

150 N. Lalaoui, A. de Poulpiquet, R. Haddad, A. Le Goff, M. Holzinger, S. Gounel, M. Mermoux, P. Infossi, N. Mano, E. Lojou and S. Cosnier, A membrane-less air-breathing hydrogen biofuel cell based on direct wiring of thermostable enzymes on carbon nanotube electrodes, *Chem. Commun.*, 2015, **51**, 7447–7450.

151 E. Lojou, M. T. Giudici-Orticoni and P. Bianco, Direct electrochemistry and enzymatic activity of bacterial polyhemic cytochromes c_3 incorporated in clay films, *J. Electroanal. Chem.*, 2005, **579**, 199–213.

152 M. Cadet, X. Brilland, S. Gounel, F. Louerat and N. Mano, Design of a highly efficient O_2 cathode based on bilirubin oxidase from Magnaporthe oryzae, *ChemPhysChem*, 2013, **14**, 2097–2100.

153 D. MacAodha, P. O Conghaile, B. Egan, P. Kavanagh and D. Leech, Membrane-less glucose/oxygen enzymatic fuel cells using redox hydrogel films containing carbon nanotubes, *ChemPhysChem*, 2013, **14**, 2302–2307.

154 S. Morozov, O. Voronin, E. Karyakina, N. Zorin, S. Cosnier and A. Karyakin, *Electrochem. Commun.*, 2006, **8**, 851–854.

155 A. Ciaccafava, P. Infossi, M. T. Giudici-Orticoni and E. Lojou, Stabilization role of a phenothiazine derivative on the electrocatalytic oxidation of hydrogen *via Aquifex aeolicus* hydrogenase at graphite membrane electrodes, *Langmuir*, 2010, **23**, 18534–18541.

156 V. Fourmond, S. Stapf, H. Li, D. Buesen, J. Birrell, O. Rüdiger, W. Lubitz, W. Schuhmann, N. Plumere and C. Leger, Mechanism of protection of catalysts supported in redox hydrogel films, *J. Am. Chem. Soc.*, 2015, **137**, 5494–5505.

157 A. Oughli, F. Conzuelo, M. Winkler, T. Happe, W. Lubitz, W. Schuhmann, O. Rüdiger and N. Plumeré, A Redox Hydrogel Protects the O_2-Sensitive [FeFe]-Hydrogenase from *Chlamydomonas reinhardtii* from Oxidative Damage, *Angew. Chem., Int. Ed.*, 2015, **54**, 12329–12333.

158 A. Ruff, J. Szczesny, S. Zacarias, I. Pereira, N. Plumere and W. Schuhmann, Protection and reactivation of the [NiFeSe] hydrogenase from *Desulfovibrio vulgaris* Hildenborough under oxidative conditions, *ACS Energy Lett.*, 2017, **2**, 964–968.

159 V. Radu, S. Frielingsdorf, O. Lenz and L. Jeuken, Reactivation from the Ni-B state in [NiFe] hydrogenase of *Ralstonia eutropha* is controlled by reduction of the

superoxidised proximal cluster, *Chem. Commun.*, 2016, **52**, 2632–2635.

160 A. de Poulpiquet, A. Ciaccafava, R. Gadiou, S. Gounel, M. T. Giudici-Orticoni, N. Mano and E. Lojou, Design of a H_2/O_2 biofuel cell based on thermostable enzymes, *Electrochem. Commun.*, 2014, **42**, 72–74.

161 T. Matsumoto, S. Eguchi, H. Nakai, T. Hibino, K.-S. Yoon and S. Ogo, [NiFe] hydrogenase from *Citrobacter* sp. S-77 surpasses platinum as an electrode for H_2 oxidation reaction, *Angew. Chem., Int. Ed.*, 2014, **53**, 8895–8898.

162 Y. Wang, T. Esterle and F. Armstrong, Electrocatalysis by H_2–O_2 membrane-free fuel cell enzymes in aqueous microenvironments confined by an ionic liquid, *RSC Adv.*, 2016, **6**, 44129–44134.

163 K. So, Y. Kitazumi, O. Shirai, K. Nishikawa, Y. Higuchi and K. Kano, Direct electron transfer-type dual gas diffusion H_2/O_2 biofuel cells, *J. Mater. Chem. A*, 2016, **4**, 8742–8749.

164 C. Lau, E. Adkins, R. Ramasamy, H. Luckarift, G. Johnson and P. Atanassov, Design of Carbon Nanotube-Based Gas-Diffusion Cathode for O_2 Reduction by Multicopper Oxidase, *Adv. Energy Mater.*, 2012, **2**, 162–168.

165 C. Narvaez Villarrubia, F. Soavi, C. Santoro, C. Arbizzani, A. Serov, S. Rojas-Carbonell, G. Gupta and P. Atanassov, Self-feeding paper based biofuel cell/self powered hybrid μ-supercapacitor integrated system, *Biosens. Bioelectron.*, 2016, **86**, 459–465.

166 T. Simmons, G. Berggren, M. Bacchi, M. Fontecave and V. Artero, Mimicking hydrogenases: from biomimetics to artificial enzymes, *Coord. Chem. Rev.*, 2014, **270**, 127–150.

167 G. Caserta, S. Roy, M. Atta, V. Artero and M. Fontecave, Artificial hydrogenases: biohybrid and supramolecular systems for catalytic hydrogen production and uptake, *Curr. Opin. Chem. Biol.*, 2015, **25**, 36–47.

168 N. Coutard, N. Kaeffer and V. Artero, Molecular engineered nanomaterials for catalytic hydrogen evolution and oxidation, *Chem. Commun.*, 2016, **52**, 13728–13748.

169 P. Rodriguez-Macia, A. Dutta, W. Lubitz, W. Shaw and O. Rüdiger, Direct comparison of the performance of a bio-inspired synthetic nickel catalyst and a [NiFe]-hydrogenase, both covalently attached to electrodes, *Angew. Chem., Int. Ed.*, 2015, **54**, 12303–12307.

170 T. Huan, R. Jane, A. Benayad, L. Guetaz, P. Tran and V. Artero, Bio-inspired noble metal-free nanomaterials approaching platinum performances for H_2 evolution and uptake, *Energy Environ. Sci.*, 2016, **9**, 940–947.

171 P. Tran, A. Morozan, S. Archambault, J. Heidkamp, P. Chenevier, H. Dau, M. Fontecave, A. Martinent, B. Jousselme and V. Artero, A noble metal-free proton exchange membrane fuel cell based on bio-inspired molecular catalysts, *Chem. Sci.*, 2015, **6**, 2050–2053.

172 S. Gentil, N. Lalaoui, A. Dutta, Y. Nedelec, S. Cosnier, W. Shaw, V. Artero and A. Le Goff, Carbon-nanotube-supported bio-inspired nickel catalyst and its integration in hybrid hydrogen/air fuel cell, *Angew. Chem., Int. Ed.*, 2017, **56**, 1845–1849.

173 D. Mersch, C.-Y. Lee, J. Z. Zhang, K. Brinkert, J. Fontecilla-Camps, A. W. Rutherford and E. Reisner, Wiring of photosystem II to hydrogenase for photoelectrochemical water splitting, *J. Am. Chem. Soc.*, 2015, **137**, 8541–8549.

174 J. Hadj-Said, M. Pandelia, C. Leger, V. Fourmond and S. Dementin, The Carbon Monoxide Dehydrogenase from *Desulfovibrio vulgaris*, *Biochim. Biophys. Acta*, 2015, **1847**, 1574–1583.

175 R. Milton, R. Cai, S. Abdellaoui, D. Leech, A. De Lacey, M. Pita and S. Minteer, Bioelectrochemical Haber-Bosch process : an ammonia-producing H_2/N_2 fuel cell, *Angew. Chem., Int. Ed.*, 2017, **56**, 2680–2683.